# Transition to detonation in fuel–air explosive clouds

## I.O. Moen

*Research and Development Branch, Department of National Defence, Ottawa,
Ontario K1A 0K2 (Canada)*

## Abstract

Several experimental observations of transition to detonation in fuel–air mixtures have clearly demonstrated that transition phenomena, similar to those identified in more sensitive fuel–oxygen mixtures, can also occur in fuel–air mixtures. This means that the worst case detonation scenario cannot be excluded *a priori* in assessing the hazards from vapour cloud explosions. The present paper describes the considerable progress that has been made towards quantifying the potential for transition to detonation in a fuel–air cloud.

## 1. Introduction

The accidental release of combustible gases or evaporating liquids can lead to devastating explosions. The most dangerous situation occurs when a combustible fuel–air cloud is formed prior to ignition. Such a cloud is most likely to burn as a deflagration, but the most severe explosion is a detonation that propagates through the detonable parts of the vapour cloud at velocities of more than 1.5 km/s producing over-pressures in excess of 1.5 MPa. Because of the large energies required to directly initiate detonations in common fuel–air mixtures, this worst case scenario is typically excluded in hazard assessments. However, during the past decade several experiments have shown that transition to detonation can occur, even in relatively insensitive fuel–air mixtures [1–7].

A sequence of photographs from an experiment which illustrates the worst case scenario is shown in Fig. 1. In this experiment, a lane 1.8 m × 1.8 m in cross-section and 15.5 m long, with an array of obstacles simulating pipes in a chemical plant, was filled with acetylene–air and then ignited by four weak sparks at one end. As the flame encounters the turbulent flow around the obstacles it accelerates, reaching a speed of about 250 m/s at Frame a in Fig. 1. Several bright spots, indicating localized explosions, can be seen within the
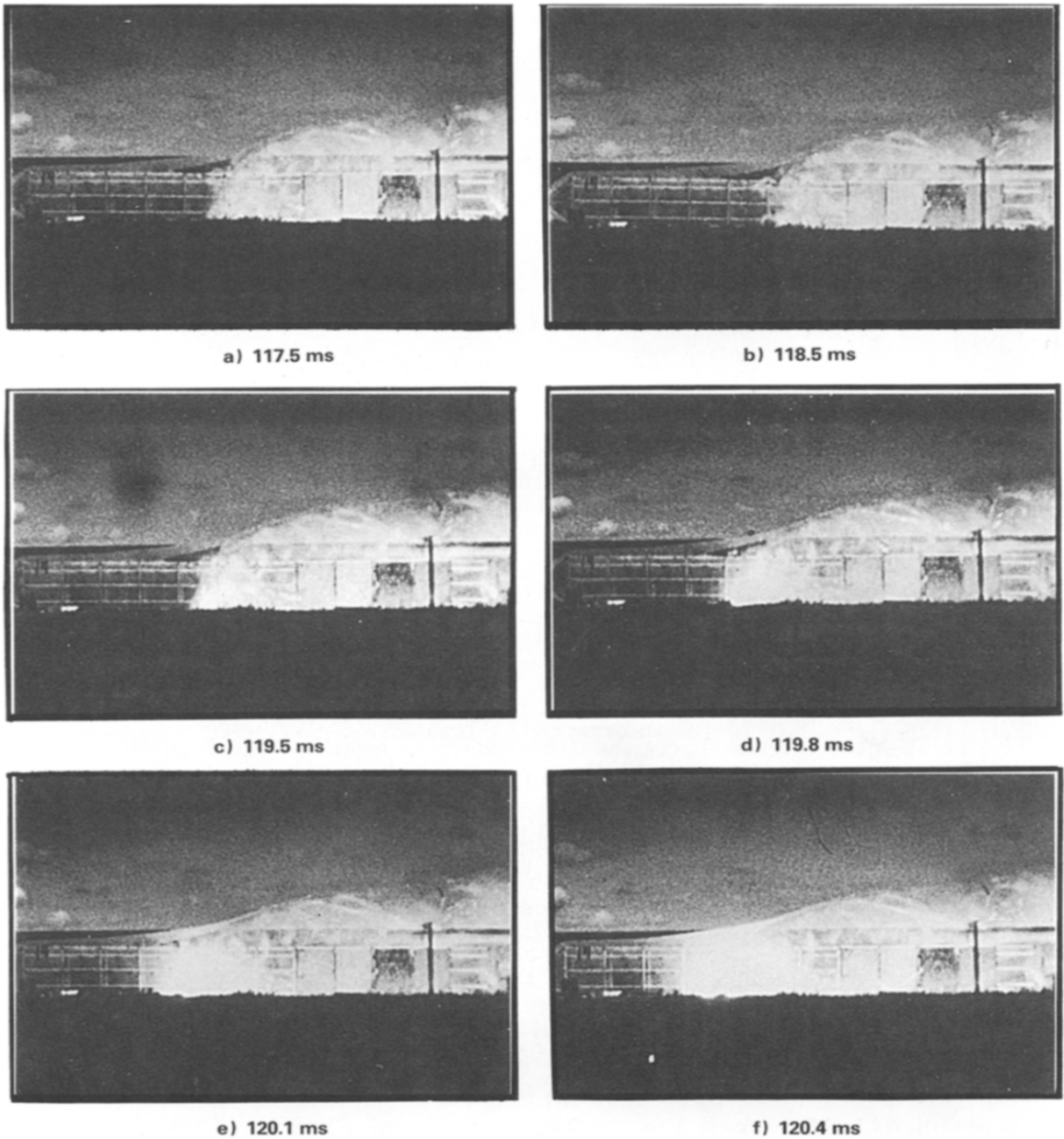
---

*Correspondence to*: I.O. Moen, Research and Development Branch, Department of National Defence, Ottawa, Ontario K1A 0K2 (Canada).

Fig. 1. Ignition, flame acceleration and transition to detonation with acetylene–air in a 1.8 m × 1.8 m lane, 15.5 m long [4].

flame brush in both Frames a and b, but it is the local explosion near the flame front in Frame c, which grows into the detonation wave seen in Frame f.

A similar transition process is revealed with good clarity in the sequence of schlieren photographs from a laboratory experiment shown in Fig. 2 [8]. The first two frames in Fig. 2 (0 and 5 μs) clearly show a fast deflagration with

# TRANSITION FROM DEFLAGRATION TO DETONATION

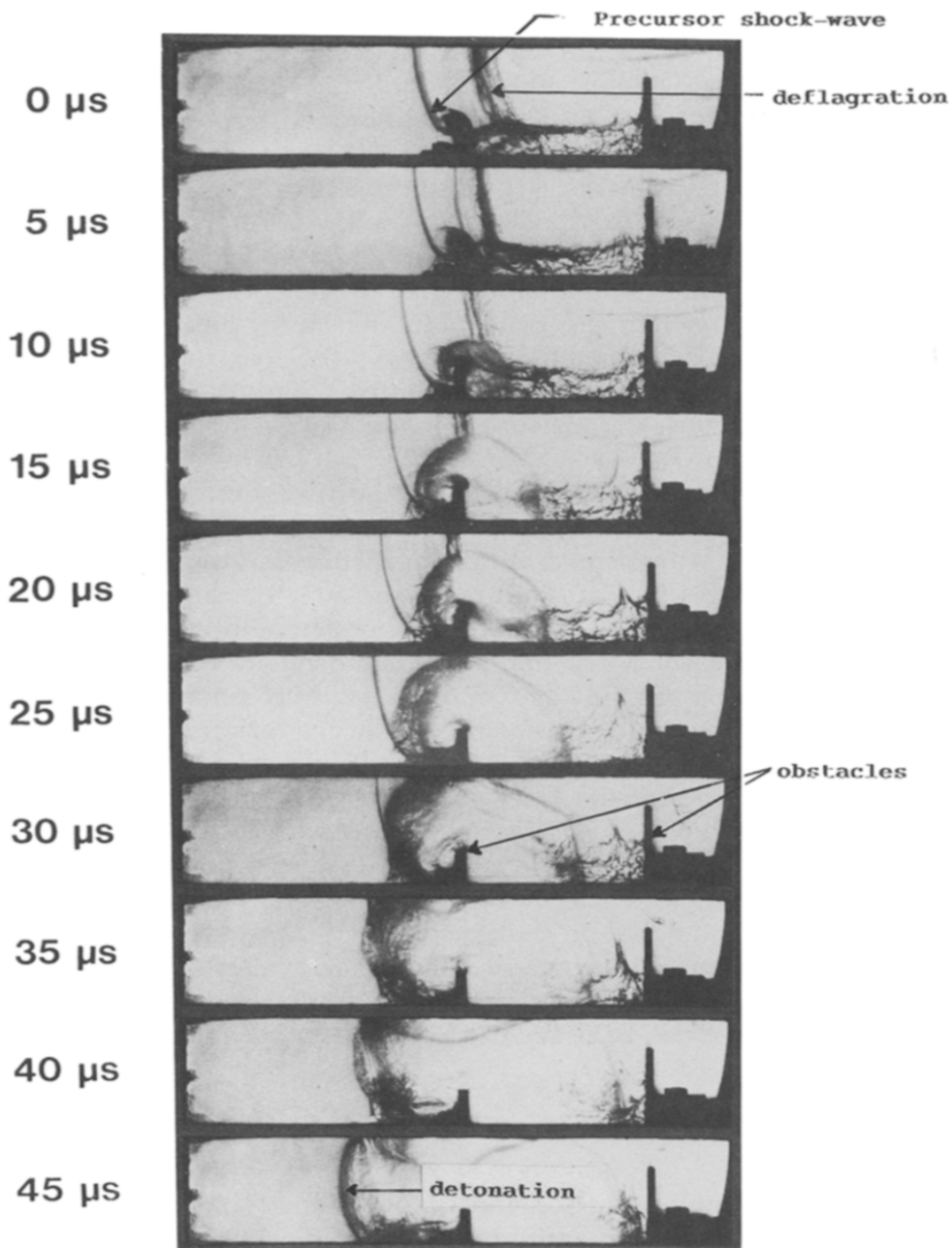## ( 2H₂ + O₂ , Pᵢ = 135 torr )



Fig. 2. Sequence of schlieren photographs illustrating the transition from deflagration to detonation phenomenon [8].

a precursor shock wave diffracting over an obstacle. A local explosion occurs at about 15 μs when the flame rolls up into the turbulent vortex ahead of the obstacle. The growth of the explosion bubble and its merger with the precursor shock wave to form a detonation wave can be seen in the subsequent frames.

These two examples show that the key feature associated with the onset of detonation is the formation of localized explosions somewhere in the turbulent frame-shock wave region. For direct initiation of detonation the initiating explosion is provided by an external high-energy source (e.g., a high explosive charge). The strong shock waves produced by such explosions directly initiate a self-sustained detonation without going through a deflagration phase.

Deflagration to Detonation Transition (DDT) refers to the phenomena where the critical conditions for the onset of detonation are established by the combustion process itself without an external high-energy source. There are several ways by which the conditions necessary for transition to detonation can be achieved. These include: (i) flame acceleration to some critical speed, (ii) ignition of a turbulent pocket, and (iii) jet ignition.

One of the proposed transition mechanisms is Shock Wave Amplification by Coherent Energy Release (SWACER) [9, 10], where the chemical energy is released in such a manner that the resulting shock waves are amplified to strengths sufficient to initiate detonation. The SWACER mechanism and other mechanisms for transition from deflagration to detonation were reviewed by Lee and Moen [11] in 1980, and more recently by Shepherd and Lee [12]. The qualitative 'picture' of the transition phenomena presented in the 1980 review paper remains essentially unchanged. However, considerable progress has been made in quantifying the flame acceleration phenomena, and in quantifying the requirements for initiation and propagation of detonations.

The aim of the present contribution is to describe some of the new developments which impact on the DDT problem. In particular, theoretical and experimental results on the nature, behaviour and initiation of gaseous detonations are reviewed. Observations of transition to detonation in fuel–air mixtures are also summarized, and the influence of mixture composition, experimental configuration and scale on flame acceleration and transition phenomena are discussed. Some of the proposed models for transition to detonation are also discussed, and proposals are made for future research to obtain a better understanding of the DDT phenomena.

## 2. General considerations

All of the complex phenomena involved in the accidental release of fuels with subsequent ignition cannot be quantified. However, a general description of the events leading to explosions can be given. The sequence of events begins with a spill of combustible fuel. If ignition occurs immediately, the result will be a diffusion flame whose rate of burning is controlled by the mixing of fuel with air. In this case, the hazards due to thermal effects from the burning

fireball are more important than the blast effects. These hazards will not be discussed here, rather we shall assume that ignition is delayed so that a potentially explosive fuel–air cloud has been formed through the mixing of the spilled fuel with air. Depending on the nature of the ignition source and the reactivity of the fuel, such a cloud can either burn as a deflagration or detonate. For a deflagration, the explosion pressure depends on the rate of combustion and the degree of confinement. Laminar flames are typically associated with low flame velocities ($\leq 10$ m/s) and small pressure changes ($\sim 1$ kPa). Completely confined explosions can produce damaging overpressures ($\sim 0.8$ MPa), and detonations produce overpressures in excess of 1.5 MPa.

Weak ignition of an explosive cloud in an unobstructed, unconfined environment is unlikely to lead to a damaging explosion. There is no mechanism for flame acceleration to high flame speeds or for producing pockets with rapid enough energy release to cause transition to detonation within such clouds. However, the influence of obstacles in the cloud can be quite dramatic, particularly repeated obstacles. Confined and partially confined regions within the cloud are also hazardous, and jet ignition from explosions in such regions can dramatically increase the severity of the explosion in an external unconfined cloud.

It is not necessary to have a detonation for severe damage to occur. In many cases, industrial structures will fail under loadings that result from fast flames. However, the damage from detonations will be much more severe and extensive; the detonation pressure is higher and the detonation will propagate through the detonable parts of the cloud at the detonation velocity, whereas the speed of a flame adjusts to the environment and will decrease to non-damaging levels in unconfined areas without obstacles.

In the present paper we are concerned with the onset of detonation from localized explosions (or regions of violent combustion) within the cloud. As will be discussed later, localized explosions can occur in the turbulent flame brush of fast flames, in the flame jet from confined explosions, and in highly turbulent burning vortices. In order for such explosions to cause the onset of detonation, a high rate of energy release in a sufficiently large volume is required. The rate of energy release and the minimum explosion volume depend on the susceptibility of the explosive mixture to detonation. The nature of detonations and methods for characterizing this susceptibility are described in the next section.

## 3. Detonation waves

### 3.1 Equilibrium detonation properties

A detonation wave can be described as a coupled reaction zone-shock wave complex which propagates through a uniform combustible mixture at a constant supersonic velocity. The shock wave heats up the mixture to a temperature above the ignition temperature, thus providing the ignition source for

the combustion to begin, and the chemical energy released in the reaction zone provides the energy required to maintain the shock wave.

The velocity of a detonation can be calculated from the total chemical energy released. The corresponding thermodynamic conditions (i.e., pressure, temperature, etc.) at the end of the reaction zone, or the so-called Chapman–Jouguet (CJ) point, can also be calculated from equilibrium chemistry alone. Standard numerical codes which combine chemical equilibrium calculations with the gasdynamic CJ conditions are available for this purpose (e.g., the NASA [13] and TIGER [14] codes). Detonation pressure ratios and velocities for some common fuel-air mixtures at stoichiometric composition are given in Table 1. Also included in this table is the chemical energy released in the detonation wave.

The equilibrium detonation parameters determine the pressure and flow field inside and outside the detonating cloud. Fairly straightforward

TABLE 1

Equilibrium detonation parameters for fuel-air mixtures (stoichiometric composition; atmospheric initial pressure, 101.3 kPa; initial temperature 298.15 K)

| Fuel | % Fuel by volume | Detonation pressure ratio | Velocity (m/s) | Energy release (MJ/kg Mixture) |
|---|---|---|---|---|
| Acetylene ($C_2H_2$) | 7.75 | 19.1 | 1864 | 2.44 |
| Hydrogen ($H_2$) | 29.6 | 15.6 | 1968 | 2.82 |
| Ethylene ($C_2H_4$) | 6.54 | 18.4 | 1822 | 2.35 |
| Ethane ($C_2H_6$) | 5.66 | 18.0 | 1825 | 2.31 |
| Propylene ($C_3H_6$) | 4.46 | 18.5 | 1809 | 2.31 |
| Propane ($C_3H_8$) | 4.03 | 18.3 | 1798 | 2.29 |
| n-Butane ($C_3H_{10}$) | 3.13 | 18.4 | 1796 | 2.28 |
| Methane ($CH_4$) | 9.48 | 17.2 | 1801 | 2.31 |
| Hydrogen sulphide ($H_2S$) | 12.3 | 15.3 | 1647 | 1.96 |
| n-Hexane | Aerosol | 18.6 | 1795 | 2.28 |

finite-difference numerical codes are available for calculating the blast field associated with ideal clouds of uniform composition. Inside such a cloud, the peak pressure is the detonation pressure, whereas the duration of the pressure pulse depends on the size of the cloud and the distance from the cloud boundaries. The far-field blast waves beyond about two cloud diameters from a detonating cloud are for all practical purposes the same as that from a TNT charge with the same energy release, located at the centre of the cloud [15].

The equilibrium detonation parameters provide no information on the detonation initiation and propagation requirements. These are determined by the structure and transient behaviour of the detonation wave.

## 3.2 Structure of detonation waves

A one-dimensional model of the detonation wave, called the Zeldovich–Von Neumann–Döring (ZND) model, includes an induction zone separating the leading shock wave and the onset of chemical reaction [16]. Although it is known that the structure of detonations is three-dimensional with waves moving transverse to the direction of propagation, the ZND model provides a useful first approximation to the detonation structure. This model has been used, together with detailed chemical kinetic models, to calculate a ZND induction zone length, $\Delta$, which is then assumed to be directly proportional to the cell size, $S$, characteristic of the cellular structure of the detonation [17–20].

The cellular structure of gaseous detonations can be attributed to instabilities in the reacting flow behind the leading shock wave. When the level of instability is relatively mild, the detonation wave consists of two families of shock waves moving in opposite directions transverse to the leading shock wave. As illustrated in Fig. 3a, the triple-point shock trajectories trace out a "fish scale" pattern, which can be recorded by placing a lightly-sooted polished metal (or mylar) foil, commonly referred to as a smoked foil, parallel to the direction of propagation. In most fuel–air systems, a large number of instability modes interact in a non-linear manner to produce a complex irregular pattern such as that shown in Fig. 3b [21]. Although the identification of a characteristic cell size is subject to some interpretation, it has been possible to identify cell sizes for many fuel–air systems from smoked foil records. Detonation cell sizes for several fuel–air mixtures at stoichiometric composition are given in Table 2. Cell size data for other compositions can be found in Refs. [22] and [23].

## 3.3 Geometric propagation and transition limits

The detonation cell size is a characteristic length scale that can be used to assess the geometric propagation and transition limits of detonations. Knystautas and co-workers [23–25] found that DDT in a round tube is possible only if the tube diameter is larger than the detonation cell size. The cell size therefore represents the minimum geometric dimension below which transition does not occur even in a completely confined tube. Similarly, a
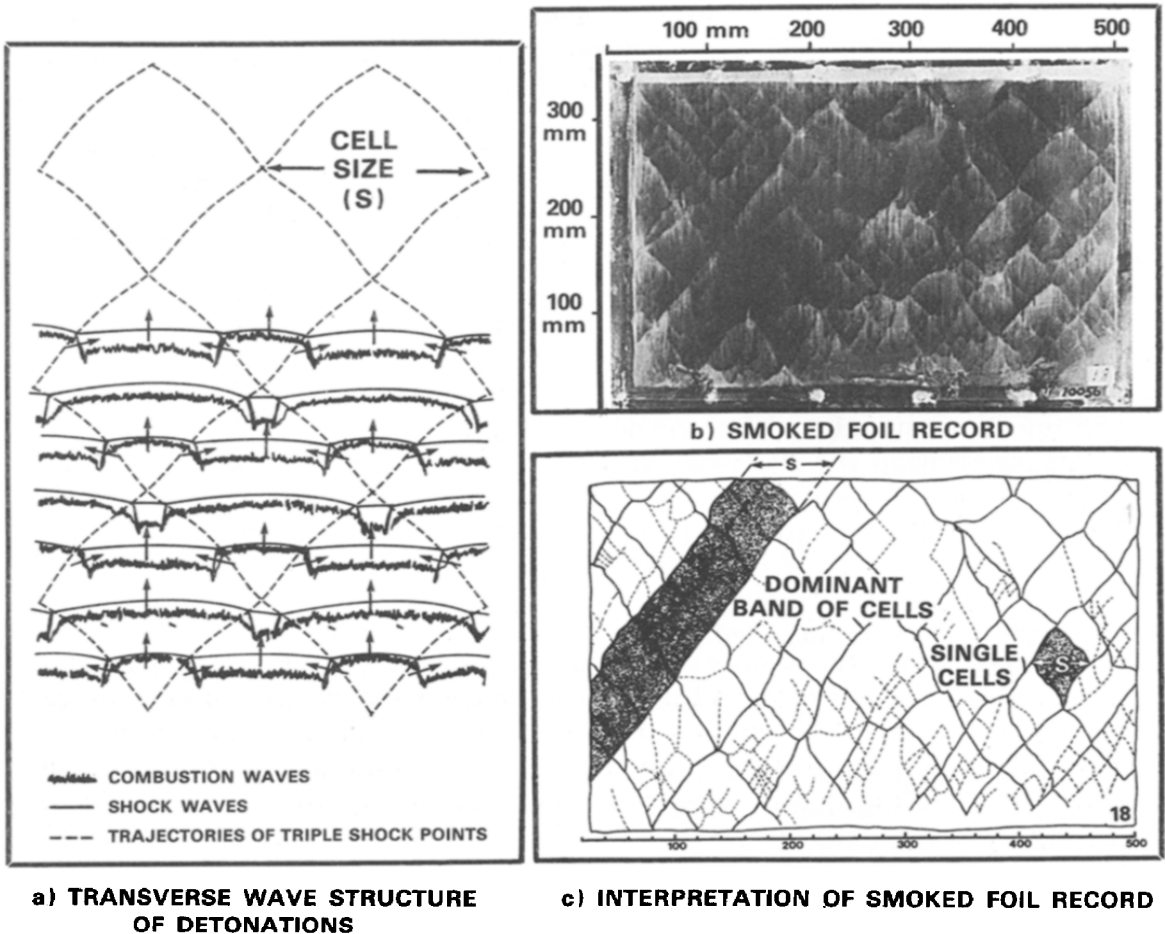
a) TRANSVERSE WAVE STRUCTURE          c) INTERPRETATION OF SMOKED FOIL RECORD
OF DETONATIONS

Fig. 3. Typical cellular structure of detonations in fuel–air mixtures [21].

detonation will fail if the tube is sufficiently small so that the transverse waves are suppressed. For systems with regular cellular structure (e.g., acetylene–oxygen highly diluted with argon), failure occurs when the tube diameter is approximately equal to the cell size. However in irregular systems, typical of fuel–air, the detonation wave merely adjusts its structure and continues to propagate in round tubes with diameters much smaller than the dominant cell size [26]. In square tubes, however, failure is observed near the cell size limit even in fuel–air mixtures [27].

A detonation wave also fails when its transverse waves are attenuated by acoustic absorbing tube walls [28]. This indicates that transverse waves are necessary for detonations to propagate. In confined tubes, the tube walls act as reflective surfaces that help to maintain the transverse waves. Once these reflective surfaces are removed, by using an absorbing material or by removing the tube walls, the detonation will fail unless the transverse wave structure can be self-supporting.

TABLE 2

Detonability parameters for fuel–air mixtures at stoichiometric composition (atmospheric initial pressure, 101.3 kPa; initial temperature 298 K)

| Fuel | Cell size (mm) | Critical tube diameter (m) | Detonation initiation energy (g Tetryl) | Critical explosion diameter (m) |
|------|------|------|------|------|
| Acetylene | 9.8 | 0.15 | 1.25 | 0.15 |
| Hydrogen | 15 | 0.2 | 1.1 | 0.16 |
| Ethylene | 28 | 0.43 | 10–15 | 0.36 |
| Ethane | 54–62 | 0.9 | 30–40 | 0.48 |
| Proplyene | 52 | — | 45–52 | 0.54 |
| Propane | 69 | 0.9 | 50–55 | 0.54 |
| n-Butane | 50–62 | 0.9 | 50–80 | 0.62 |
| Hydrogen sulphide | 90–130 | — | — | — |
| Methane | 250–310 | — | 22 000 | 4.0 |

The first observation that a minimum tube diameter is required for a detonation wave to emerge from a tube and become a detonation in an unconfined cloud was made by Zeldovich et al. [29]. This minimum or critical tube diameter, $d_c$, is a measure of the minimum dimension of an unconfined detonable cloud. Experimentally, this dimension is between 10–30 detonation cell widths, depending on the explosive mixture. For most fuel–air mixtures, $d_c \simeq 13S$ [22, 26].

The critical tube diameter is determined from "Go–No Go" experiments, in which the fate of the detonation is monitored as it emerges from a tube into an unconfined explosive cloud. Selected frames from high-speed photographic records illustrating successful transmission and failure to transmit from 0.9 m diameter tube are shown in Fig. 4. The first frames of both sequences show the planar detonation wave just as it emerges from the tube. The initial planar detonation core shrinks (Frames 2 and 3) as the expansion waves sweep in towards the centre. For successful transmission, re-ignition is seen to occur at nuclei near the center in Frame 3. The subsequent formation of a detonation wave which sweeps through the pre-shocked region just outside the central core of burned gas can be seen in Frame 4. This detonation wave engulfs the whole region in Frame 5. In the case of detonation failure, no ignition nuclei are formed and the detonation is quenched when the head of the expansion wave reaches the centre at about one tube diameter from the tube exit.

The critical tube diameters for several fuel–air mixtures at stoichiometric composition are given in Table 2. The values range from 0.1–0.2 m for acetylene– and hydrogen–air mixtures to almost 1 m for propane–, ethane– and butane–air mixtures. Critical tube diameters for other compositions can be found in Refs. [22] and [23].
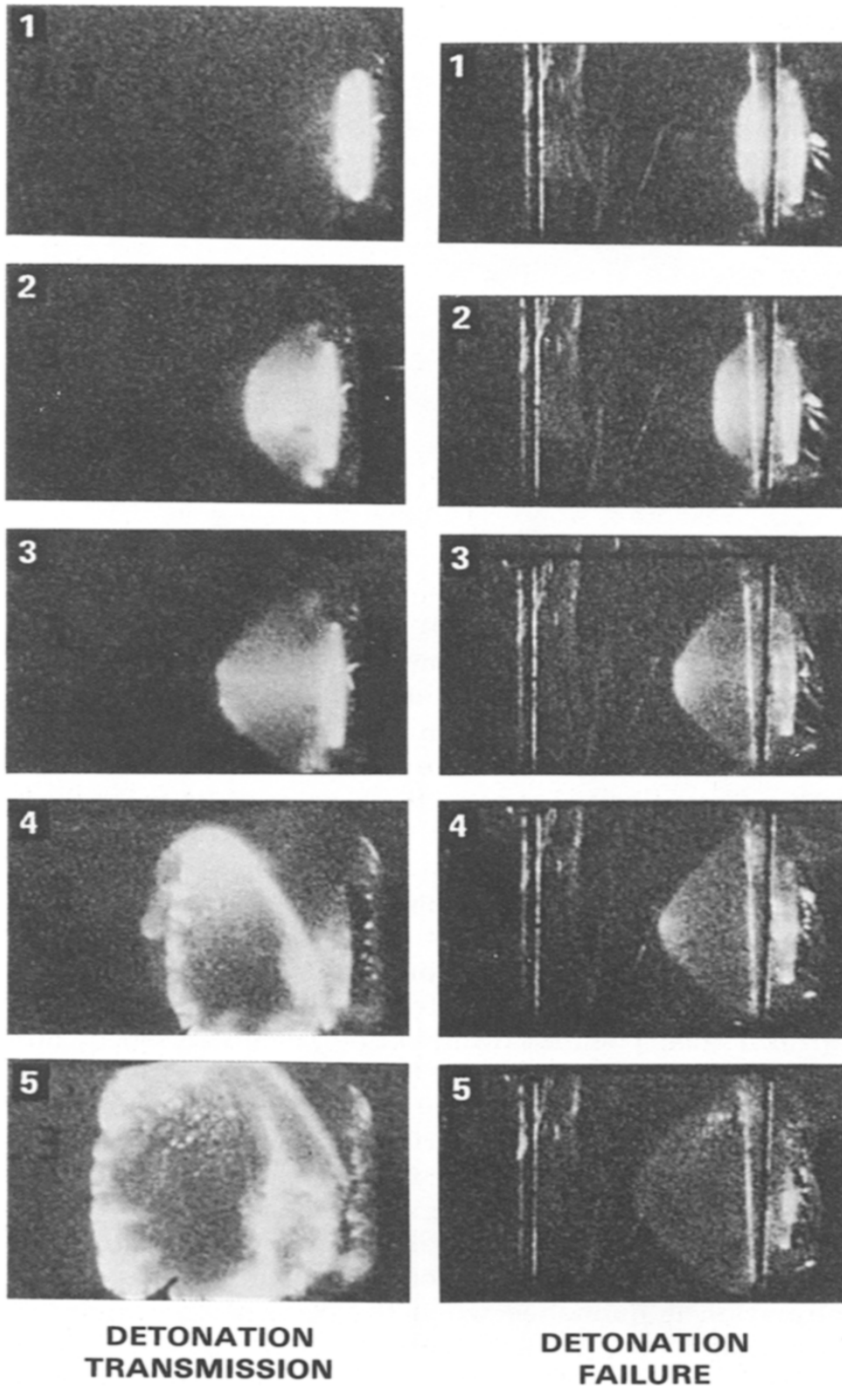
Fig. 4. Selected frames from high-speed photographic records illustrating successful transmission and failure when a detonation emerges from a 0.9 m diameter tube.

## 3.4 Direct initiation of detonation

The detonation length scales $S$ and $d_c$ provide a measure of how large an explosive cloud must be in order to support a detonation. A minimum quantity of energy is required to establish a detonation wave in this explosive cloud. For unconfined fuel–air clouds, the critical initiation energy is usually characterized by the minimum mass of high-explosive required to initiate a spherical detonation wave. Bull [30] proposed that tetryl be used as the high-explosive standard. The equivalent energy of tetryl is approximately 4.3 MJ/kg. Unless otherwise specified we shall adopt this standard and use this energy equivalency.

Experimental values of the critical initiation energy for several fuel–air mixtures at stoichiometric composition are given in Table 2. The initiation requirements vary from 1 g of tetryl for hydrogen and acetylene fuels to several kilograms for methane. For common fuels such as propane and butane, the detonation initiation requirements are about 50 g of tetryl.

For most fuel–air mixtures, the variation in critical initiation energy with composition takes the form of a U-shaped curve with a minimum near stoichiometric composition. This is illustrated in Fig. 5, where the critical initiation energies for selected fuel–air systems are plotted vs. the equivalence ratio $\phi$, where $\phi$ is the volume ratio of fuel to air relative to that at stoichiometric composition.

The earliest theoretical concept of critical initiation energy is due to Zeldovich and co-workers [29]. Their concept still remains the simplest and most direct. The rapid release of energy results in a decaying blast wave. The heuristic limiting condition proposed for successful initiation is that at least one chemical induction time must have elapsed before the blast wave Mach number has decayed to the CJ value. For spherical geometry, this assumption leads to the relationship $E_c \propto \Delta^3$, between the critical energy, $E_c$, and the ZND chemical induction zone length, $\Delta$. Numerous refinements and re-interpretations of the theory of initiation have been developed, but the fundamental concept remains unchanged. All the models predict that $E_c \propto L_c^3$ where $L_c$ is one of the chemical length scales (i.e., $\Delta$, $S$ or $d_c$). If it is also assumed that the chemical length scales are linearly related, it is then possible to determine the variation of detonability with composition through chemical kinetic calculations [17–19]. Some indication of the reliability of such estimates can be obtained by referring to Fig. 6, where $E_c$ is plotted vs. $d_c$. The general $E_c \propto d_c^3$ trend is valid for a given fuel. However, the proportionality factor for acetylene–air is almost 20 times larger than that for ethane–air.

In summary, a fairly good qualitative understanding of detonations and detonability properties has emerged during the past decade. This understanding, together with the empirical relationships that have been derived from a large pool of new data, has provided a good background against which the DDT problem can be addressed.
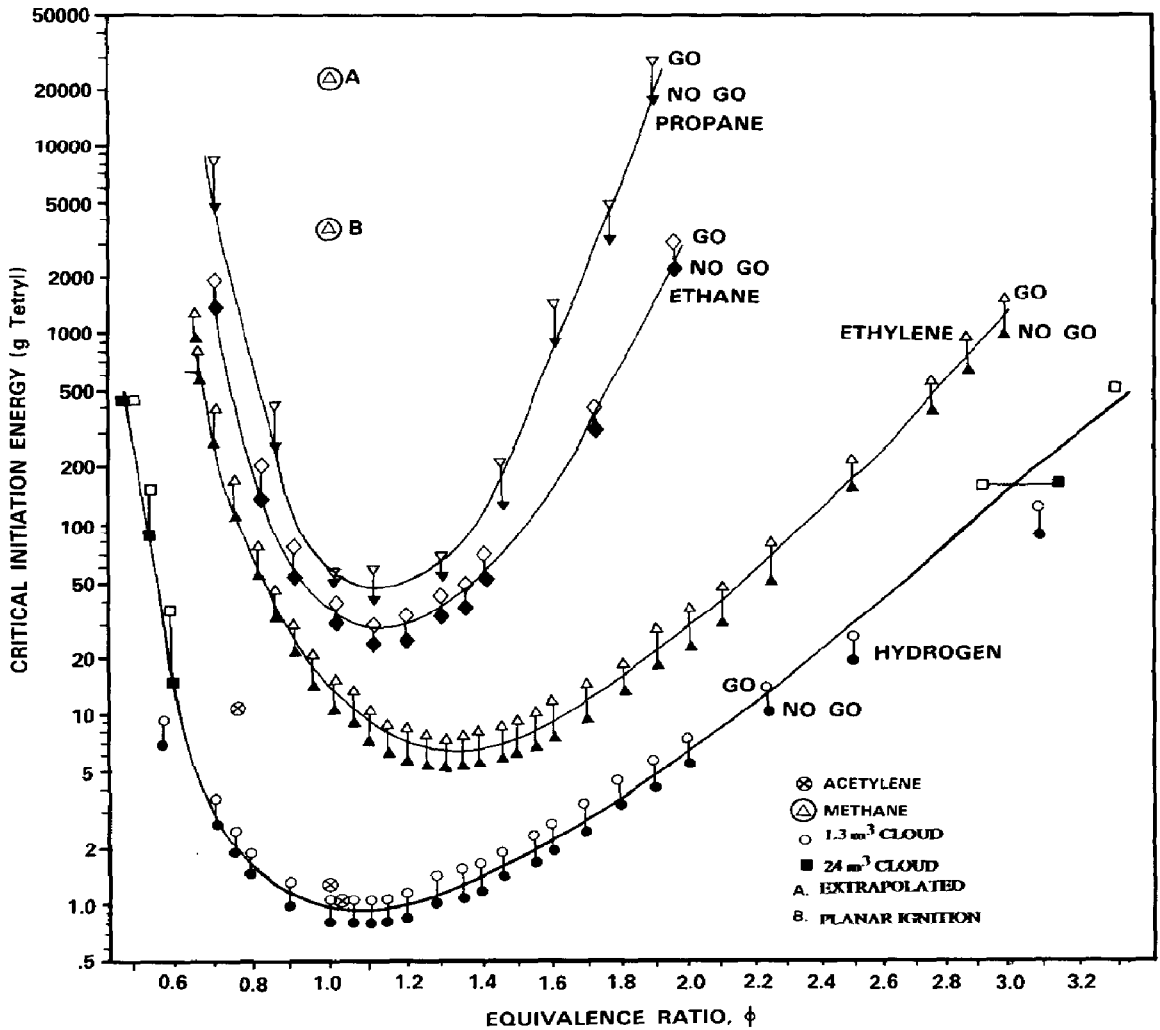
Fig. 5. Critical initiation energy vs. equivalence ratio, $\phi$, for selected fuel–air mixtures [30, 31].

# 5. Transition to detonation

## 5.1 Mechanisms and criteria

Transition to detonation is the onset of detonation in a combustible mixture without an external high energy source. In this case, the energy required to initiate detonation is provided by combustion of the mixture. This "self-initiation" requires a rapid release of combustion energy to produce a blast wave of sufficient strength to cause detonation. As described by Lee and Moen [11], such shock waves can be produced by prescribing a spatial and temperal coherence of the energy release. Theoretically, the required coherence can be achieved by pre-conditioning the explosive mixture so that the induction time
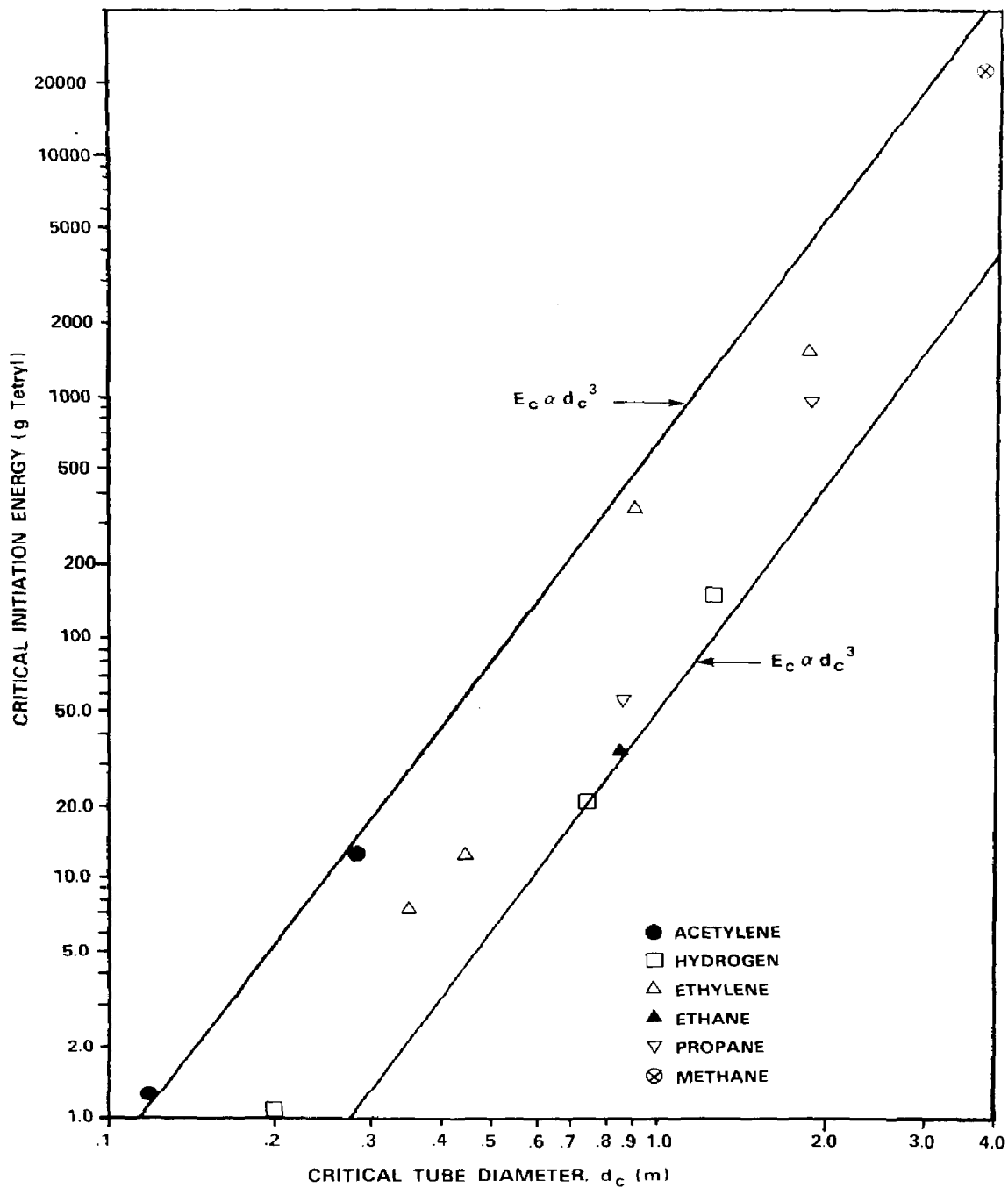
Fig. 6. Critical initiation energy vs. critical tube diameter.

$\tau$ (i.e., time to ignition) increases in a prescribed manner away from an initial ignition point to produce an energy source which propagates at a velocity $V_0 = (\partial\tau/\partial x)^{-1}$. Numerical calculations indicate that a source velocity close to the Chapman–Jouguet detonation velocity produces the best shock wave amplification [11].

Spatial gradients in induction time are due to gradients in temperature and/or free radical concentrations. The so-called SWACER mechanism was first proposed to account for photochemical initiation in $H_2 + Cl_2$ mixtures [9]. In these experiments, the induction time gradient was produced by irradiating the explosive mixture with a strong short-duration flash. Photo-dissociation thus produces a gradient in free radical concentration (Cl) which decreases exponentially in the direction of the incident light.

Gradients in temperature and free-radicals are also produced by turbulent mixing of hot combustion products with unburned gas in turbulent eddies associated with flame propagation around obstacles or in turbulent flame jets. It was Knystautas et al. [10] who first demonstrated that initiation of detonation could be achieved by injecting a hot turbulent jet into a quiescent explosive fuel–oxygen mixture.

Coherent energy release by itself is not enough for transition or detonation, the volume of coherent energy release must also be large enough to produce a strong enough shock wave with long enough duration to initiate detonation in the surrounding unburned mixture. A lower bound on the volume required for transition to occur in an unconfined cloud can be obtained by equating the chemical energy in a spherical volume to the critical initiation energy by an external source:

$$E_c = \pi\rho_0 QD_c^3/6, \tag{5.1}$$

where $Q$ is the chemical energy release per unit volume, $\rho_0$ is the density of the unburned mixture, and $D_c$ is the critical explosion diameter. This diameter is of the same order of magnitude as the critical tube diameter (see Table 2). Critical diameters for fuel–air mixtures are at least an order of magnitude larger than for fuel–oxygen, so that field experiments are required to clarify the potential for DDT in unconfined fuel–air clouds.

There are several ways by which the conditions necessary for transition to detonation can be achieved. These include: (i) flame acceleration to some critical speed, (ii) ignition of a turbulent pocket, and (iii) jet ignition. In the remainder of this section we will discuss these, but first let us make some general observations.

A wide variety of experiments, both large and small scale, have been performed so that there is now a considerable data base on flame acceleration and transition to detonation in fuel–air mixtures. The results prior to 1986 have been summarized and compiled in a report by Moen and Saber [32]. Particularly hazardous configurations were identified as those which are heavily confined. In tubes, pipes and confined channels, for example, high flame speeds and pressures are reached within less than four diameters, even in insensitive

mixtures of methane and air. Similar flame acceleration is also observed in clouds confined on top and bottom. Such clouds could be produced by a release into an area which is covered by a roof. Explosions in confined spaces can also serve as strong ignition sources for external clouds, greatly enhancing the potential for DDT. Weak spark ignition of unconfined clouds in a relatively unobstructed environment is unlikely to result in transition to detonation or damaging explosions, even for sensitive fuel–air mixtures such as acetylene– and hydrogen–air. However, transition can be expected to occur in long channels or tubes for most fuel–air mixtures, provided the channel or tube is large enough and long enough.

## 5.2 Flame acceleration

One method of creating the conditions necessary for transition to detonation is flame acceleration to some critical speed. Flame acceleration is particularly dramatic in repeated obstacle environments. In such environments, the flame is repeatedly perturbed, so that a positive feed-back mechanism is established, resulting in high flame speeds after only a short distance of flame travel.

The mechanisms of transition in fast turbulent flames were revealed with unsurpassed clarity by the stroboscopic laser–schlieren photographs of Urtiew and Oppenheim [33]. Their photographs clearly show that localized explosions somewhere between the precursor shock wave and the end of the turbulent flame brush lead to the onset of detonation. An example of onset of detonation due to a localized explosion immediately behind the precursor shock wave is shown in Fig. 7.

In order for transition to occur, sufficiently high flame speeds must be reached. The flame speeds observed prior to the rapid acceleration phase, characteristic of the transition phase, are between 500 and 800 m/s [24, 25, 34]. Since most flame acceleration mechanisms are very effective in confined tubes, acceleration of the flame to speeds sufficient to cause onset of detonation can be expected, provided the tube is long enough. Transition to detonation will then occur if the detonation cell size is not larger than the tube diameter. The run-up or transition distance depends on many factors, including: fuel–air mixture, tube diameter, ignition source, obstacles, etc. In stoichiometric hydrogen–air, for example, the transition distances observed by Bartknecht [35] in smooth tubes are 7.5–12.5 m, whereas Knystautas et al. [25] observe transition just after a 3 m long obstacle section. The transition distance observed in pipes was reviewed by Steen and Schampel in 1983 [36]. In pipes with no obstacles, the transition distance increases with increasing tube diameter. In propane–air mixtures, for example, the transition distance was found to be about 8 m in a 50 mm diameter pipe and more than 30 m in a 400 mm diameter pipe.

Flame propagation in tubes has been studied experimentally by several authors [24, 25, 34–39], and Hjertager and co-workers [39–42] have developed numerical methods for describing the flame acceleration phenomena in tubes, with and without obstacles. The actual mechanisms responsible for DDT in tubes are not understood so that transition cannot be predicted *a priori*, but
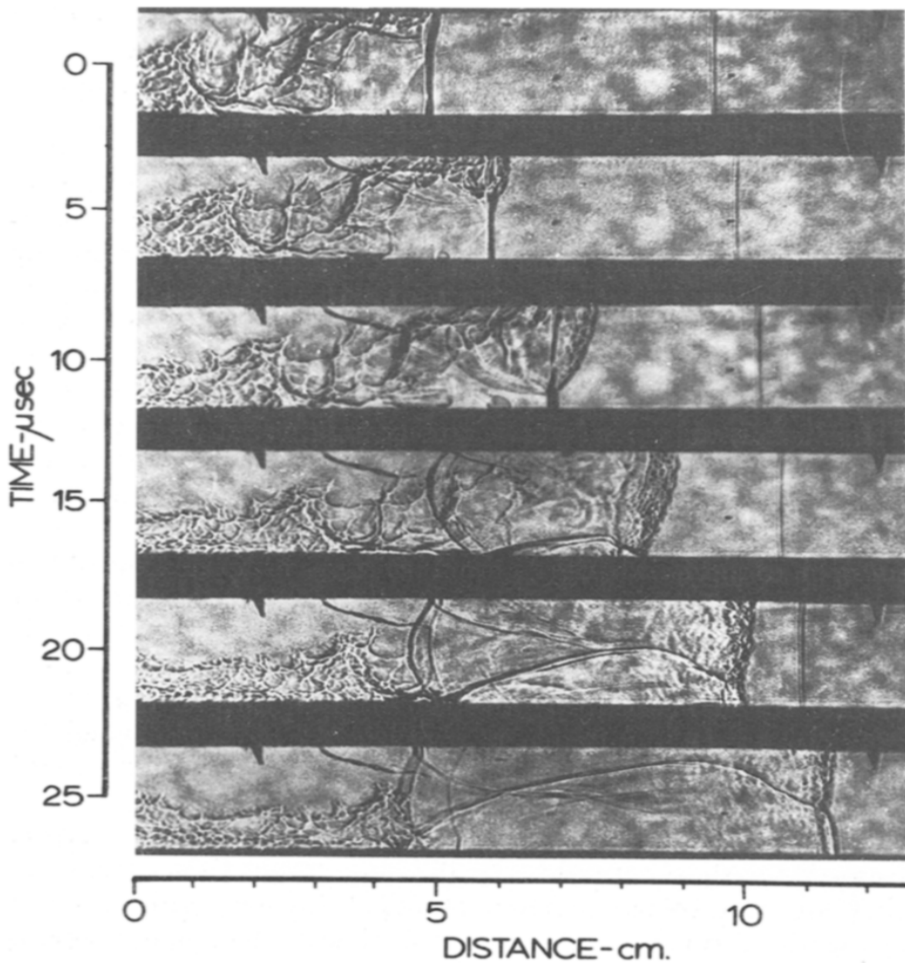
Fig. 7. Stroboscobic schlieren record of the onset of detonation in a low pressure hydrogen/oxygen mixture, with localized auto-explosion immediately behind the precursor shockwave at about 5 µs [33].

tube configurations which produce flame speeds in excess of 500 m/s can be expected to lead to the onset of detonation in mixtures whose detonation cell size is less than the tube diameter. Long tubes or channels therefore represent the most hazardous configurations for DDT. The consequences of such transitions will be particularly devastating if the detonation is transmitted into a large external cloud. As discussed in Section 3.3, this will occur if the tube diameter is greater than the critical tube diameter.

Flame acceleration and transition phenomena were studied on a relatively large scale at SANDIA in their FLAME apparatus (a channel 30.5 m long, 2.4 m high and 1.8 m wide) designed to investigate hydrogen combustion relevant to nuclear reactor safety [3, 43]. Transition to detonation was observed in

near-stoichiometric hydrogen–air mixtures with no obstacles for a closed-top channel and with 13% top venting. However, with 50% of the top of the channel open, continuous flame acceleration leading to transition to detonation was not observed.

The results from the FLAME experiments confirm that the flame acceleration and transition phenomena observed on a smaller scale also occur on a large scale. They also show that the degree of confinement plays an important role in controlling the flame acceleration. This is consistent with the laboratory results obtained by Chan et al. [44] in an investigation on the influence of top venting on flame acceleration in a channel with repeated obstacles. They found that the maximum flame speed of 350 m/s with a closed top decreased to 5 m/s when 50% of the top was open. A similar influence of top venting on flame acceleration was also observed by Van Wingerden and Zeeuwen [45] in their pipe-rack obstacle arrays. These results show that the flame acceleration and thus the possibility of transition to detonation is reduced significantly by removing confinement.

The first observations of transition to detonation in large partially confined clouds were made by Pförtner et al. [1, 46], who used a fan to generate tubulence in a hydrogen–air cloud contained in an open-top lane, 3 m × 3 m in cross-section and 10 m long. With no obstacles or turbulence generators, the maximum flame speed was 200 m/s, with an associated maximum pressure of 20 kPa. However, when a fan (1.25 m in diameter at 225 rpm) was placed 1 m from the ignition end to generate turbulence, transition to detonation occurred about 2 m downstream of the fan.

Transition to detonation following flame acceleration in a lane with repeated obstacles was observed by Moen et al. [4, 47]. This phenomena was described in the Introduction. The test section was a channel 1.8 m × 1.8 m in cross-section, 15.5 m long, confined on three sides with a plastic envelope covering the top. The obstacle arrays consisted of 500 mm or 220 mm diameter pipes mounted across the channel at regular intervals as illustrated in Fig. 8. Experiments were performed with acetylene, propane and hydrogen sulphide fuels.

The potential for flame acceleration and transition to detonation is clearly illustrated by the results obtained in near stoichiometric acetylene–air mixtures. For these mixtures, the flame accelerates down the channel and reaches speeds between 250 and 400 m/s prior to the occurrence of localized explosions which trigger the onset of detonation. The flame velocity and peak overpressure observed as the flame propagates down the channel are shown in Fig. 9. With the larger (500 mm) obstacles, the leading flame front reaches the end of the channel with a velocity of about 400 m/s, at which time an explosion near the bottom of the channel triggers detonation of the remaining unburned mixture. Also shown in Fig. 9 are the results of numerical calculations (for the larger obstacles) using a $k$–$\varepsilon$ turbulence model, which incorporates turbulent combustion through a mixing model limited by a single-step induction time [40–42].
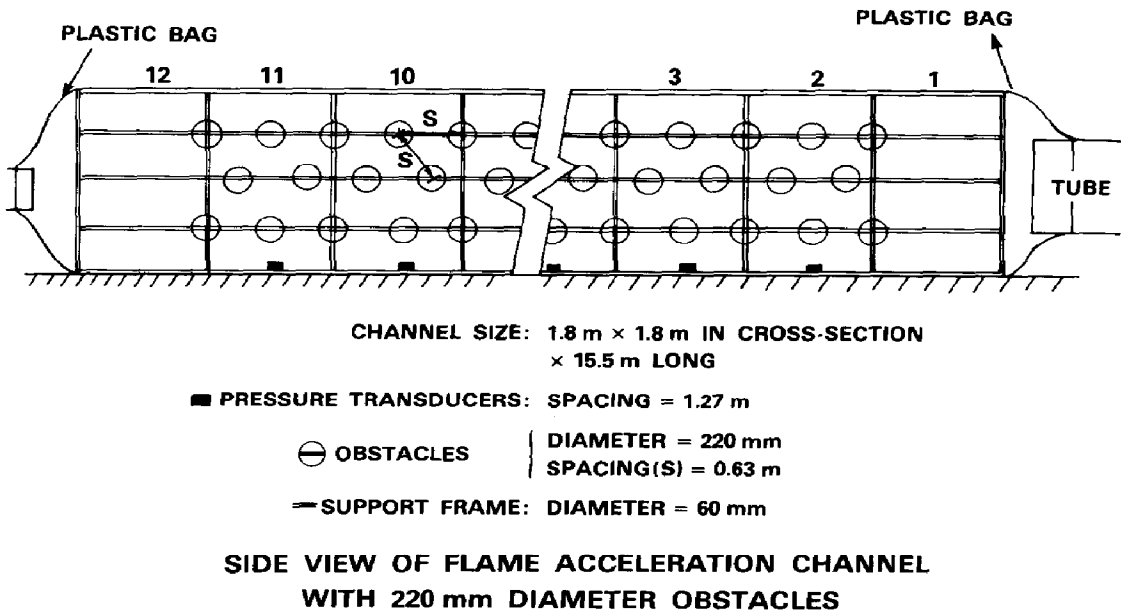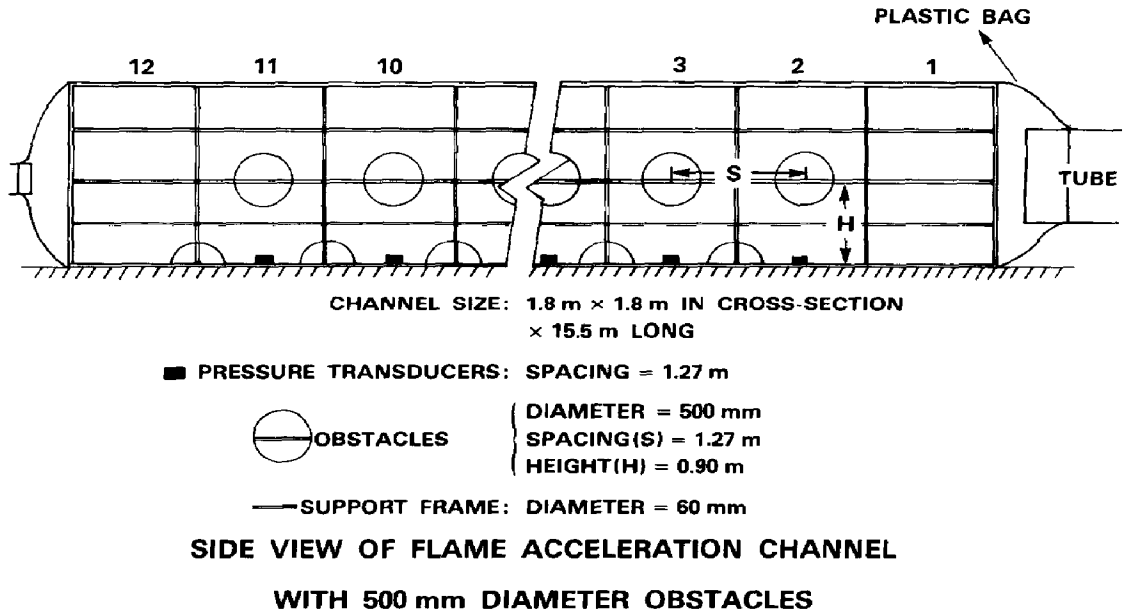
CHANNEL SIZE: 1.8 m × 1.8 m IN CROSS-SECTION
× 15.5 m LONG

■ PRESSURE TRANSDUCERS: SPACING = 1.27 m

⬭ OBSTACLES
DIAMETER = 500 mm
SPACING (S) = 1.27 m
HEIGHT (H) = 0.90 m

——SUPPORT FRAME: DIAMETER = 60 mm

**SIDE VIEW OF FLAME ACCELERATION CHANNEL**

**WITH 500 mm DIAMETER OBSTACLES**



CHANNEL SIZE: 1.8 m × 1.8 m IN CROSS-SECTION
× 15.5 m LONG

■ PRESSURE TRANSDUCERS: SPACING = 1.27 m

⊖ OBSTACLES
DIAMETER = 220 mm
SPACING (S) = 0.63 m

—SUPPORT FRAME: DIAMETER = 60 mm

**SIDE VIEW OF FLAME ACCELERATION CHANNEL**
**WITH 220 mm DIAMETER OBSTACLES**

Fig. 8. Flame acceleration channel with: 500-mm diameter obstacles; and 220-mm diameter obstacles [4, 47].

With the smaller 220 mm obstacles, transition to detonation occurs about 11 m down the channel, again due to a localized explosion at ground level. The flame speed reaches about 250 m/s prior to a rapid acceleration phase which starts 9 m down the channel and results in a full-fledged detonation with
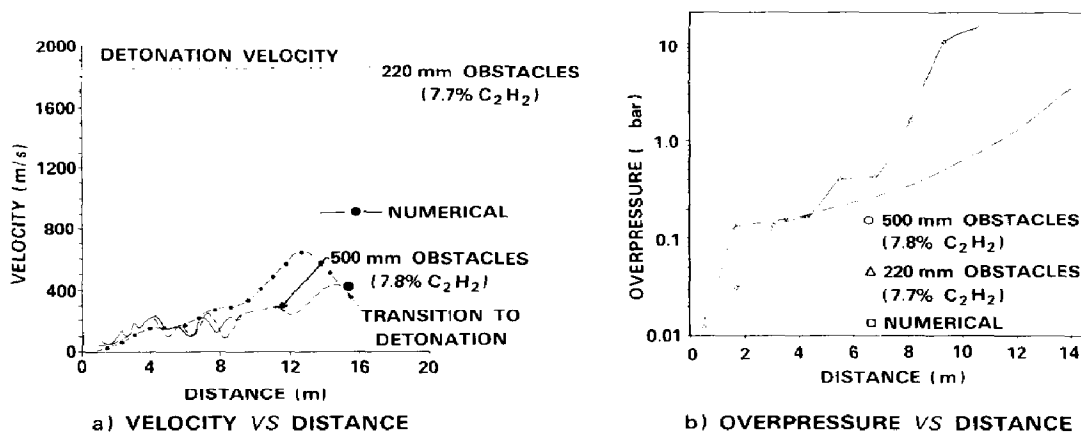
Fig. 9. Experimental and numerical results for acetylene–air mixtures: (a) flame velocity vs. distance; (b) peak overpressure vs. distance [4, 47].

a velocity close to the theoretical value by the end of the channel (see Fig. 9a). Prior to the rapid acceleration phase, the peak pressure is less than 2 bar (0.2 MPa). The peak pressure quickly increases to a detonation-like pressure of about 15 bar (1.5 MPa) at 10.6 m (see Fig. 9b). Selected frames from a high-speed film record showing the flame propagation and transition to detonation are shown in Fig. 1, and described in the Introduction.

The behaviour of flames in propane– and hydrogen sulphide–air mixtures in the same lane with repeated obstacles is much less dramatic. The flame speeds range from about 25 m/s up to 200 m/s, with associated pressures typically less than 5 kPa. The flame speeds observed in propane–air mixtures are up to four times larger than the maximum flame speed observed in the same mixtures in a similar laboratory scale channel (0.9 m long by $0.3 \times 0.15 \, m^2$) with repeated obstacles [48].

Similar results are reported by Harris and Wickens [7] in a larger open-sided rig (3 m × 3 m in cross-section and 45 m long) with a similar array of obstacles. Using an 18 m length of the test section, they obtain maximum flame speeds of 70 m/s in cyclohexane–air, 65 m/s in butane–air and 50 m/s in natural gas air, with associated maximum pressures between 3 and 7 kPa. In ethylene–air, flame speeds of over 200 m/s were recorded and maximum pressures were up to 80 kPa. By extending the length of the test section to the full 45 m with obstacles throughout, flame speeds of 230 m/s with pressures up to 70 kPa were recorded in cyclohexane–air. The corresponding values for natural gas–air were 80 m/s and 10 kPa. These values are somewhat higher than those predicted by scaling the results of Moen et al. [4, 47] using the numerical model of Hjertager and co-workers [40, 42]. As seen in Fig. 10, the peak explosion pressure is predicted to increase with scale, but for a channel scaled up by a factor of about 3 in length, the peak pressure in propane–air is predicted to be less than 0.1 bar (10 kPa). Yet these pressure levels are observed in a much less sensitive mixture of natural gas and air.
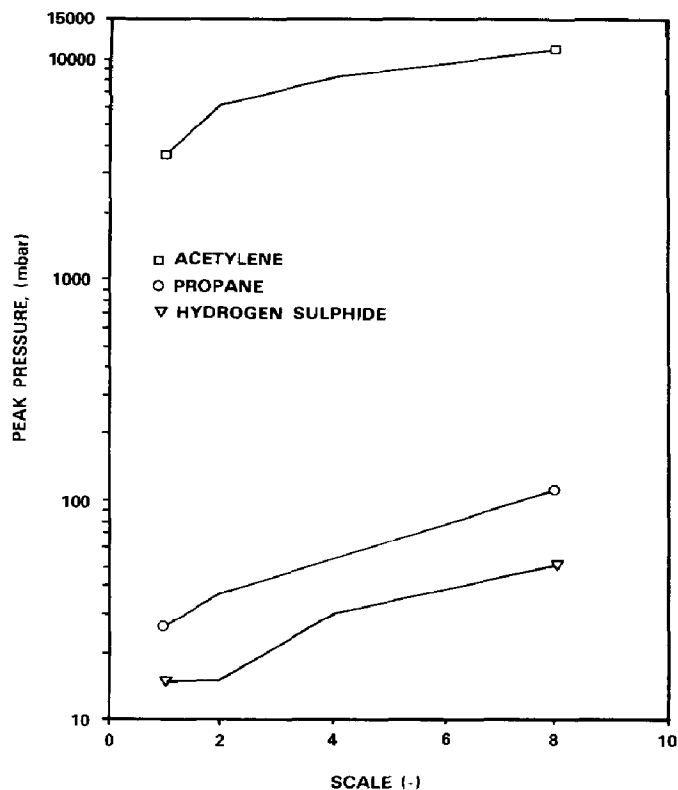
Fig. 10. Variation of peak pressure with linear scale. Scale of one corresponds to 1.8 m × 1.8 m cross-section channel, 15.5 m long, with 500-mm diameter obstacles [4].

Nevertheless, the scaling predictions shown in Fig. 10 indicate that transition to detonation is unlikely in mixtures such as propane–air in configurations with similar obstacle densities, ignition source and confinement to the experimental configuration used by Moen et al. [4, 47]. The fact that flames in acetylene–air and hydrogen–air do produce detonations in such partially confined environments show that the potential for very damaging explosions does exist. However, in order for such explosions to occur in less sensitive mixtures, the cloud must be: (i) more highly confined; (ii) ignited by a strong ignition source (e.g., strong ignition from a confined explosion); (iii) in a denser obstacle environment; or (iv) highly turbulent prior to ignition.

Transition to detonation in propane–air has been observed in highly confined vessels, and by strong ignition from a confined explosion. Bjørkhaug and Hjertager [6] observed transition to detonation in propane–air in a 10 m radial vessel, confined on the top and bottom, with central ignition, and with obstacles blocking 50% of the area between the plates. Harris and Wickens [7] report transition to detonation in propane–air mixtures in their 45 m-long test rig with obstacles when the first 9 m of the rig is covered with solid walls to produce an initial rapid acceleration of the flame. However, transition to

TABLE 3

Transition to detonation in fuel–air mixtures by flame acceleration in partially confined configurations

| % Fuel by volume | $d_c$ (m) | $V_f$[a] (m/s) | Configuration | $V_{max}$[b] (m/s) | $P_{max}$[c] (bar) | Reference |
|---|---|---|---|---|---|---|
| Hydrogen ($H_2$) 24.8% | 0.23 | 14.2 | 30.5 m × 2.4 m × 1.8 m 13% Top venting | 230 | 0.65 | Sherman et al. [3] |
| Hydrogen ($H_2$) 36 & 38% | 0.23 | 21.9 23.2 | 10 m × 3 m × 3 m Open-top lane with fan | 220 240 | 1.0 | Pförtner et al. [1] |
| Acetylene ($C_2H_2$) 7.8% | 0.12 | 12.1 | 15 m × 1.8 m × 1.8 m Open top lane with obstacles | 435 375 | >0.15 | Moen et al. [4, 47] |
| Cyclohexane ($C_6H_{12}$) 2.3% | — | 3.6 | 45 m × 3 m × 3 m Open-sided lane with obstacles | 600 | — | Harris and Wickens [7] |
| Propane ($C_3H_8$) 4.0% | 0.9 | 3.7 | 45 m × 3 m × 3 m Open-sided lane with obstacle (first 9 m of lane confined) | 600 | — | Harris and Wickens [7] |
| Propane ($C_3H_8$) 4.0% | 0.9 | 3.7 | 10 m radial vessel with obstacles | 500 | — | Bjørkhaug and Hjertager [6] |

[a] Laminar flame speed assuming velocity of burned gas is zero.
[b] Maximum flame speed prior to transition to detonation.
[c] Maximum overpressure prior to transition.

detonation in natural gas–air was not observed even with a flame speed of 1000 m/s in the confined region.

The reported observations of transition to detonation in large partially confined fuel–air clouds by flame acceleration are summarized in Table 3. Flame speeds just prior to ignition range from about 230 m/s in hydrogen–air mixtures to between 500 and 600 m/s for propane–air and cyclohexane–air mixtures.

*5.3 Ignition of a turbulent pocket*

Another mode of transition to detonation was observed by Moen et al. [4, 47] in one of their experiments with acetylene–air in the open-top lane with repeated obstacles. In this experiment, the turbulent pocket at the end of the channel was ignited by a hot wire used to cut the plastic. The phenomena is illustrated in Fig. 11 by a sequence of frames from a high-speed film record. The turbulent burning in the end-pocket (Frames a and b) produces an explosion near ground level (Frames c and d) that leads to a detonation prior to the arrival of the main flame front.
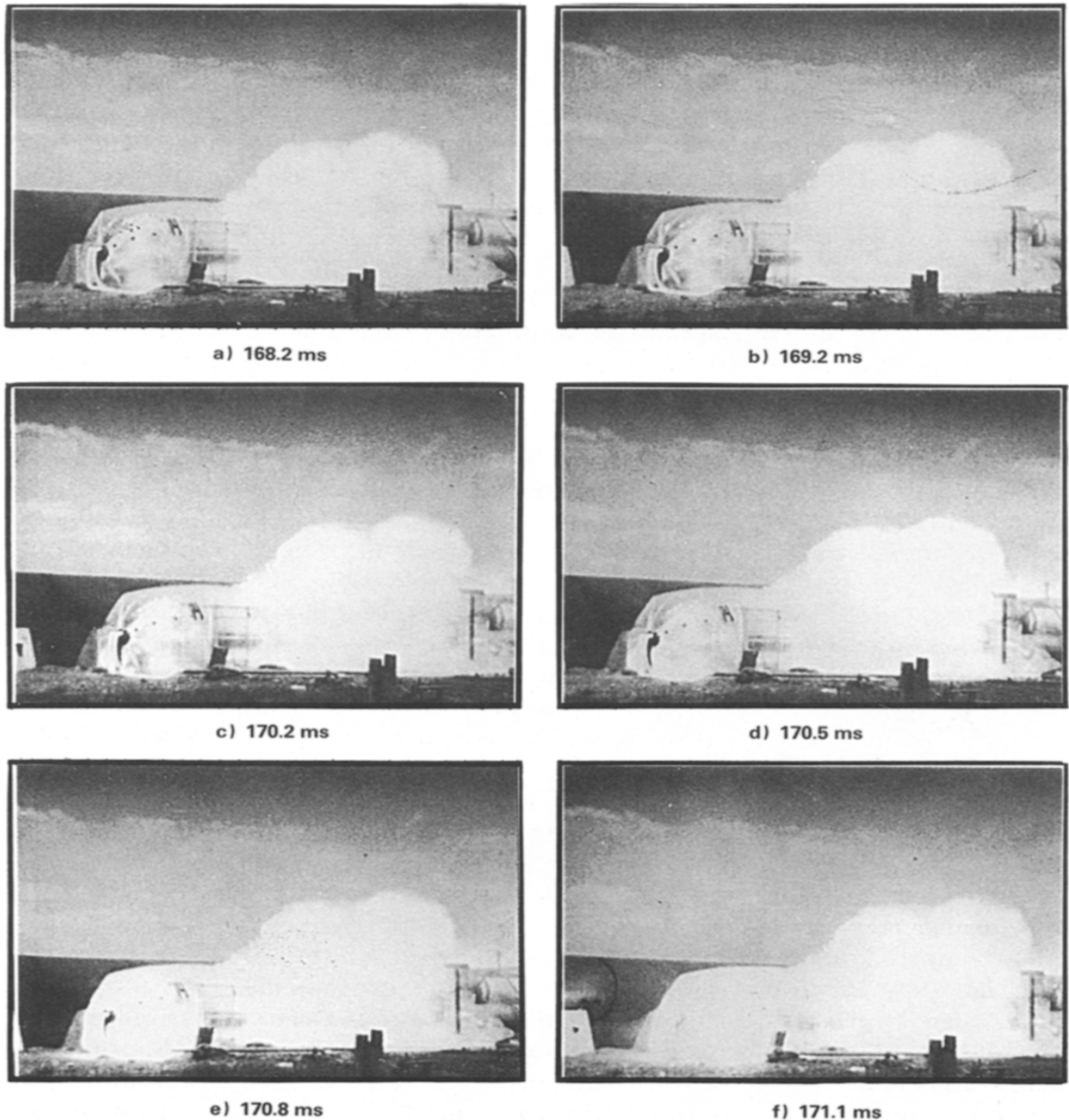
Fig. 11. Selected frames from high-speed film record showing explosion and transition to detonation in a turbulent end-pocket of acetylene–air prior to the arrival of the main flame front [4, 47].

The maximum velocity of the main flame front, prior to the onset of detonation, was 180 m/s with an associated overpressure of 13.2 kPa. Such pressures are much too small for shock reflections to be responsible for the onset of detonation. However, the flame-induced flow produces a pocket of turbulent

flow at the end of the channel. It is the ignition of this pocket which triggers an explosion of a sufficiently large volume to cause transition to detonation.

A similar transition to detonation phenomenon in a less sensitive mixture (5% $C_2H_2$–air), was observed in a jet-ignition experiment [2]. In that experiment, a fast flame emerging from a 0.64 m diameter tube produced violent turbulent burning in a cloud contained in a 2 m diameter plastic bag. Selected frames from a high-speed movie showing flame propagation, explosion, and transition to detonation are included in Fig. 12. The trajectories of the flame and detonation fronts are plotted in Fig. 13. The first frame in Fig. 12 shows the flame just as it emerges from the tube. The next frame shows the flame 2 ms later. The flame is highly turbulent and unstable, with a flame tongue running ahead at a speed of about 600 m/s near the bottom of the bag. This flame tongue reaches the lower corner at the end of the bag about 5.4 ms after the flame emerges from the tube. The resulting burning in this corner is seen in Frames c and d. In Frame d, a curled up flame vortex can be seen in the corner. The type of burning seen in these last two frames incubates for about 1.2 ms, at which time a localized explosion occurs in the corner (Frame e). The subsequent growth of an explosion bubble into a detonation front propagating backwards along the bottom of the bag can be seen in Frames f and g. As seen in Frame h, the resulting detonation wave engulfs the remaining unburned gas in the bag.

These two observations show that the gradients in temperature and free radicals required for transition to detonation can be established in turbulent eddies or pockets. In both cases, the turbulent eddies are produced ahead of the main flame front and transition to detonation occurs before the main flame front arrives. One of the observations is for a relatively insensitive mixture of 5% acetylene in air, with a critical tube diameter of 0.6 m and a minimum detonation initiation energy of about 20 g of tetryl high-explosive. Both hydrogen and ethylene can produce fuel–air clouds which are more sensitive to detonation, and there is no reason to exclude similar transition to detonation in less sensitive mixtures provided the turbulent pocket is large enough.

## 5.4 Jet ignition

The first demonstration that the conditions for onset of detonation can be achieved by turbulent mixing between hot combustion products and unburned mixture was made by Knystautas et al. [10]. In their experiment a turbulent jet of combustion products was injected into a cloud of explosive mixture. A sequence of schlieren photographs illustrating the transition to detonation in the flame jet is shown in Fig. 14. The turbulent structure of the hot jet of combustion products is clearly evident in the first four frames (10–95 µs). At 114 µs, a detonation "bubble" resulting from an exploding eddy somewhere within the turbulent mixing region can be seen. This bubble expands and eventually sweeps the entire surface of the turbulent region to form a detonation.

The jet initiation experiments of Knystautas et al. were performed with an initial flame jet diameter of 40 mm, and various turbulence inducing obstacles
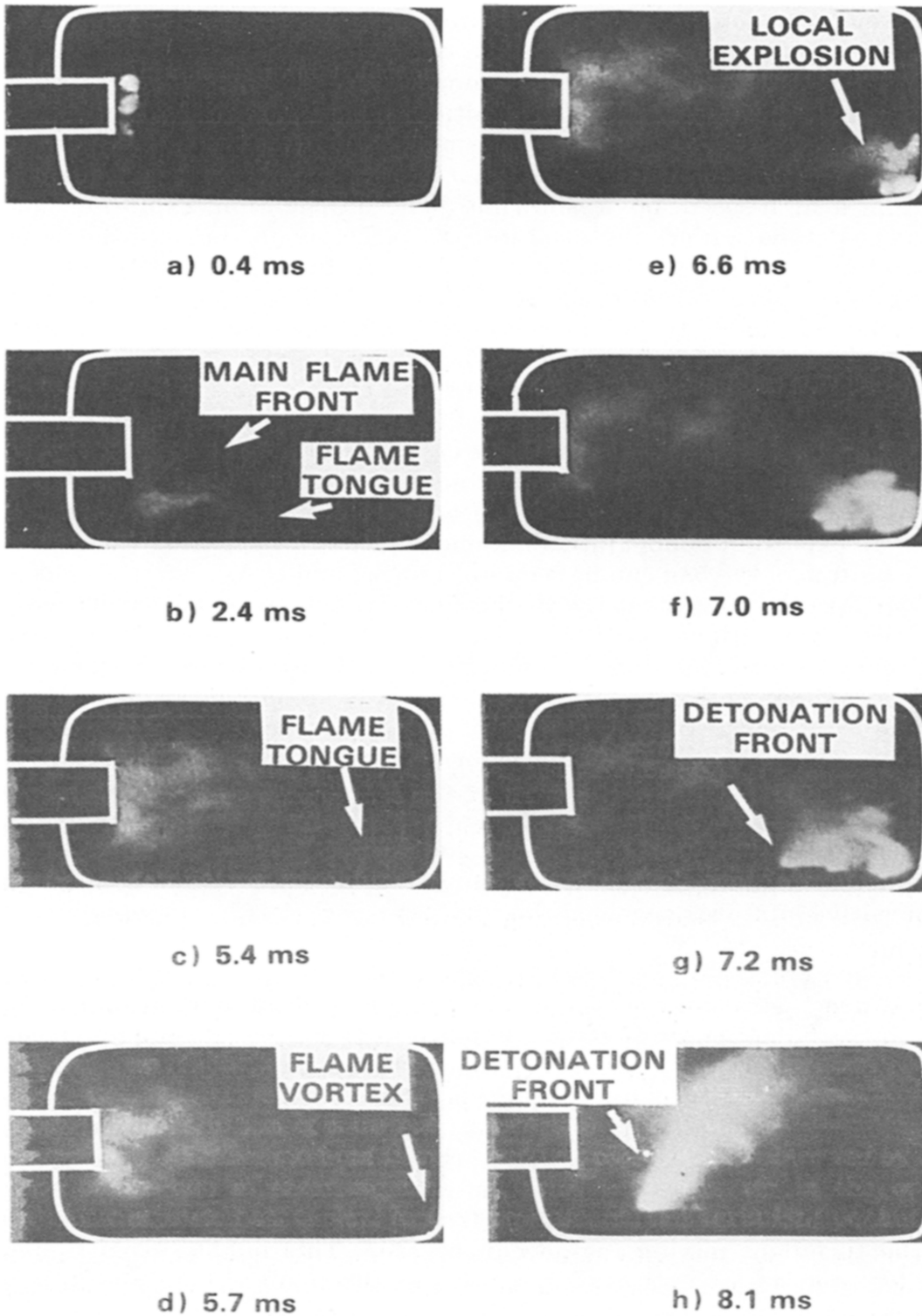
Fig. 12. Flame propagation and transition to detonation in a 2 m diameter plastic bag with ignition by a flame jet emerging from a 0.64 m diameter tube (5% v/v, $C_2H_2$–air) [2].
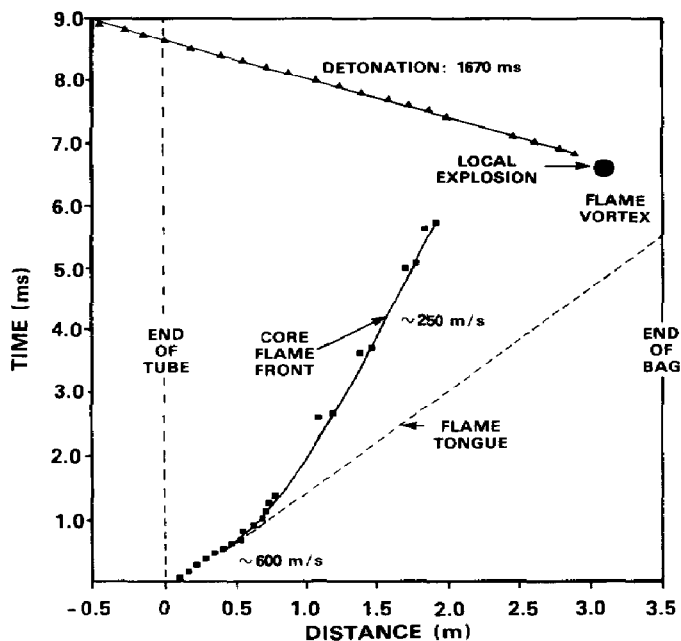
Fig. 13. Trajectories of the flame and detonation fronts in 5% $C_2H_2$–air mixture ignited by a flame jet [2].

in the orifice plate connecting the flame chamber and the larger detonation chamber. Detonation was obtained in equimolar acetylene–oxygen at an initial pressure of 150 torr. The critical tube diameter for this mixture at this pressure is about 5 mm. The smallest critical tube diameter of fuel–air mixtures is about 80 mm for rich acetylene–air. Based on linear scaling with the critical tube diameter, a minimum jet diameter of about 0.6 m would therefore be required in order to begin observing similar jet initiation phenomena in fuel–air mixtures.

In an investigation of flame-jet ignition in acetylene–air clouds, Moen et al. [5] confirmed that transition also occurs in fuel–air flame jets provided the scale is large enough. The first series of experiments were performed at a large-scale, fuel–air facility at Raufoss, Norway. The experimental configuration consisted of a 0.66 m diameter steel tube, 11 m long, connected to a large plastic bag 2 m in diameter (see Fig. 15). Experiments were performed with the end of the tube connected to the plastic bag completely open, partially blocked by circular discs with diameters 0.55 m and 0.36 m, and with an orifice plate (50 mm holes, open area ratio 0.25).

An example of transition to detonation in a flame jet from an open tube is shown in Fig. 16. In this case, the flame accelerates down the tube producing a flame jet with an exit velocity of almost 600 m/s. The intense turbulent burning in the jet can be clearly seen in the first two frames (0.33 and 1.33 ms). The intensity of the burning appears to increase in the next frame (2.33 ms). At
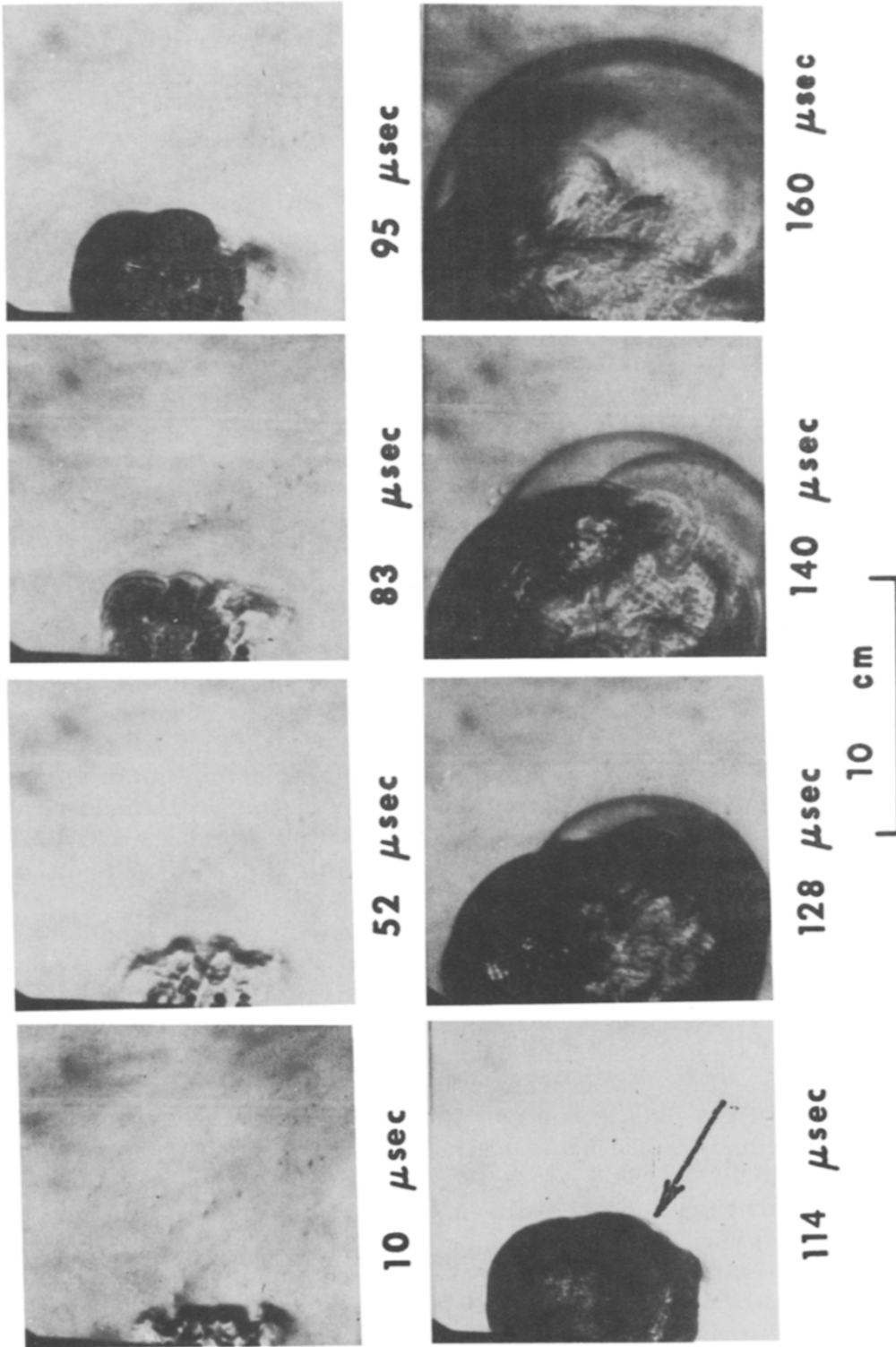
Fig. 14. Sequence of spark schlieren photographs showing the initiation of detonation by turbulent mixing with a hot turbulent jet of combustion products. The mixture is equimolar $C_2H_2 + O_2$ at an initial pressure $P_O = 150$ torr [10].
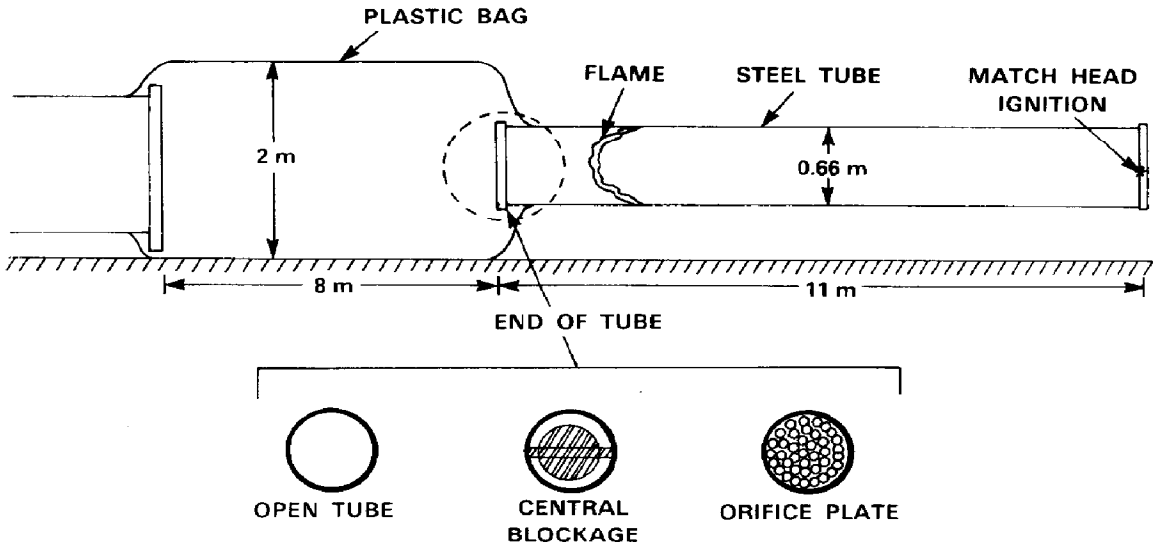
Fig. 15. Sketch of experimental configuration for investigation of flame jet ignition of acetylene–air clouds [5].

2.67 ms, a localized explosion near the tube exit leads to the onset of detonation. This detonation then propagates through the remaining unburned mixture in the bag.

The second series of jet ignition experiment were performed at the Defence Research Establishment (DRES) Fuel–Air Explosive facility [49]. The experimental configuration that was filled with explosive gas is shown in Fig. 17. It consisted of a 7.8 m long tube, 0.9 m in diameter, with a 1.8 m (or 2.4 m) diameter plastic bag, 8 m in length, attached to the open end of the tube. The end of the tube attached to the plastic bag was either unobstructed or partially blocked by a central circular disc 0.43 m or 0.58 m in diameter. Various arrays of obstacles were used to accelerate the flame which was ignited by a spark at the closed end of the tube. The test fuels were acetylene, ethylene, propane and vinyl chloride monomer.

Transition to detonation in the flame jet was observed for a range of acetylene–air concentrations and flame jet velocities. A plot of the flame jet velocity, $V_j$, versus mixture sensitivity expressed in the form $d_c/D$, where $d_c$ is the critical tube diameter of the mixture and $D$ is the tube diameter, is shown in Fig. 18. The data indicate that a minimum velocity of about 600 m/s is required for initiation in the most sensitive fuel–air mixtures ($d_c/D \simeq 0.1$). This minimum $V_j$ increases as the mixture sensitivity decreases. At $d_c/D \simeq 0.5$, for example, the minimum flame jet velocity is about 700 m/s.

Some of mechanisms which can trigger transition to detonation were identified from the high speed film records. They include a variety of flame/vortex, flame/flame and flame boundary interactions, some of which are illustrated in the flame and detonation front contours shown in Fig. 19.
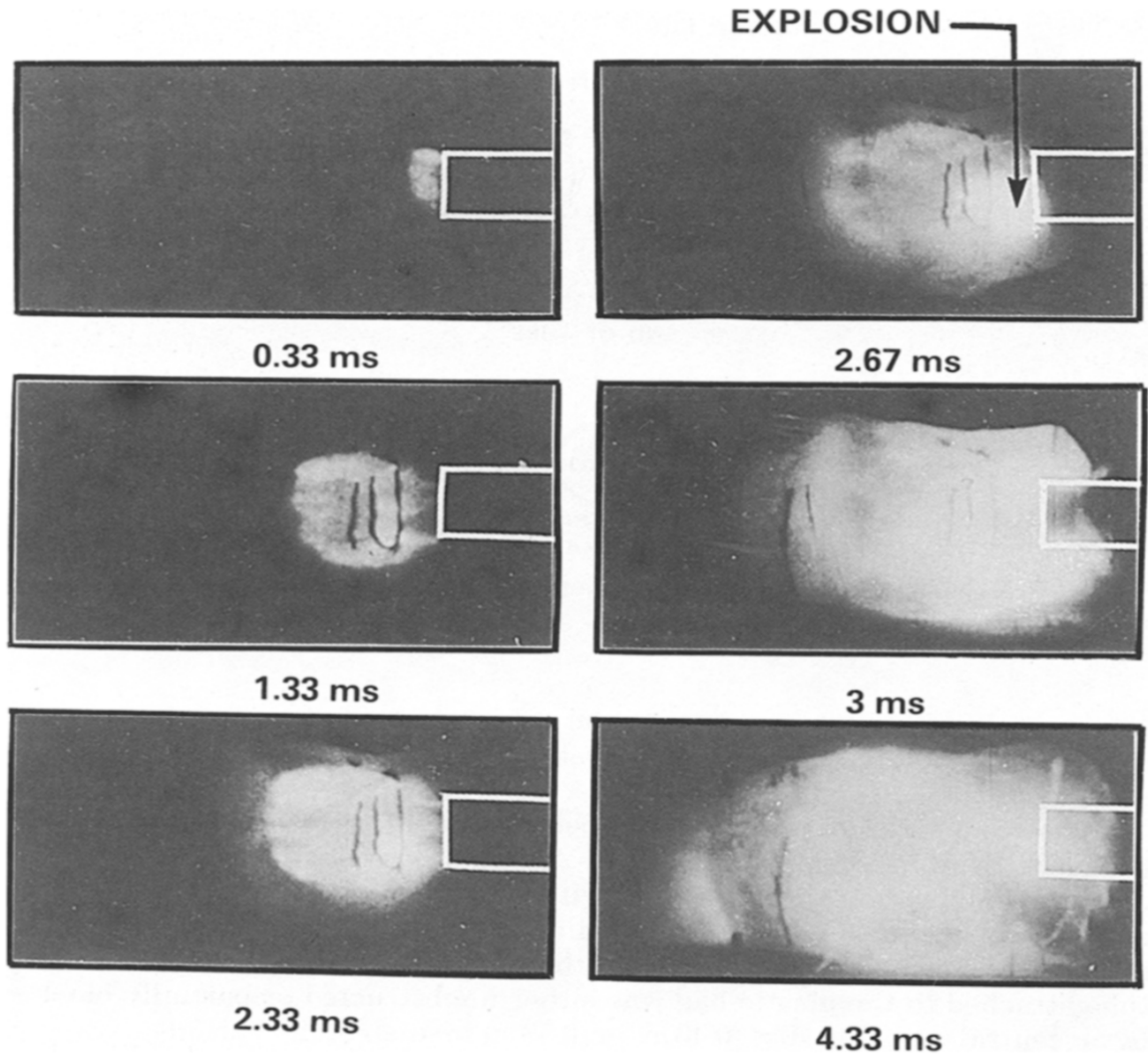
Fig. 16. Sequence from high-speed film showing transition to detonation in the flame jet (7.9% $C_2H_2$) from an open 0.66-m diameter tube, 11 m long [5].

With etylene–, propane– or vinyl chloride–air mixtures, the critical conditions for transition were not realized in the outside cloud. The flame-jet velocities were too low for transition to occur in these less sensitive mixtures. Even though transition to detonation does not take place, violent explosions were observed in ethylene–air mixtures producing overpressures in excess of 0.5 MPa in the outside cloud, significantly larger than the maximum pressure in the tube.

In summary, the results of these large scale jet ignition tests confirm that the phenomena of transition to detonation in fuel–air mixtures are identical to those in fuel–oxygen mixtures, but on a much larger scale due to the less
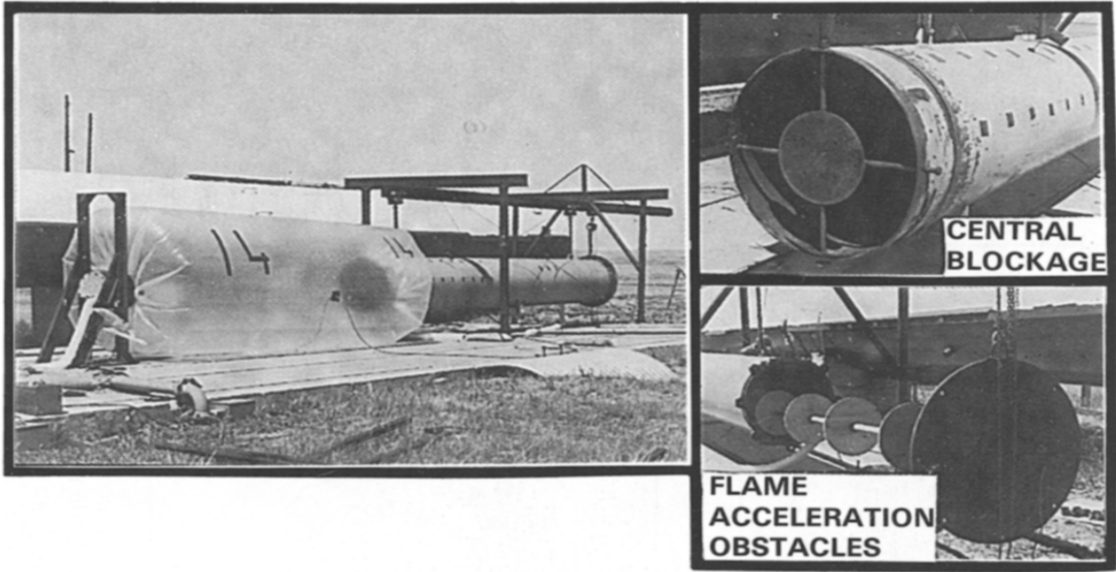
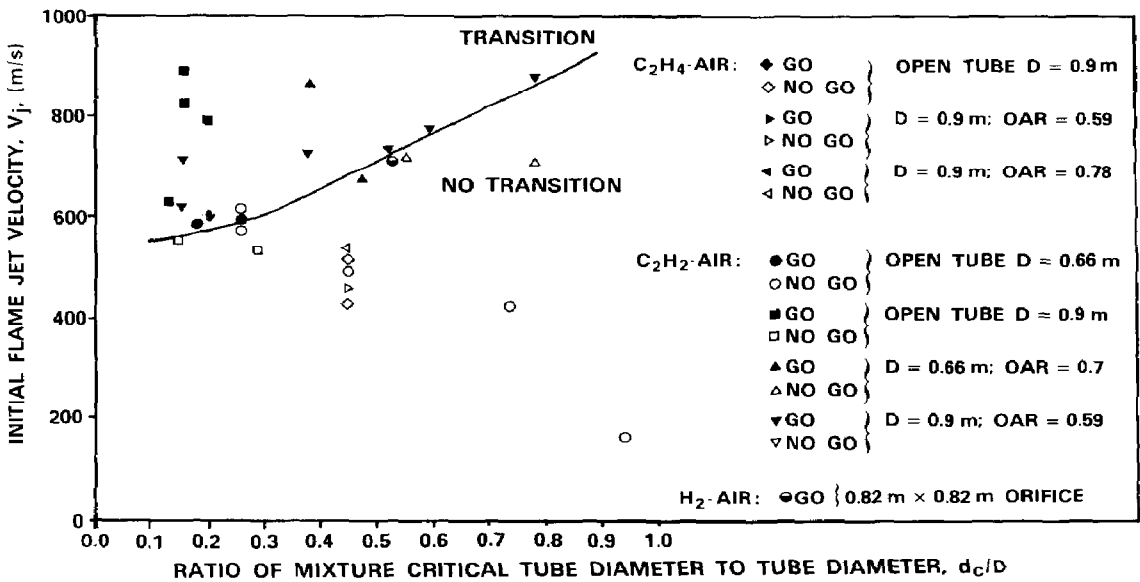Fig. 17. The experimental apparatus used in flame-jet initiation studies [49].



Fig. 18. Plot of initial flame jet velocity against the sensitivity of the mixture to detonation. (Tube diameter $D = 0.66$ m from Ref. [5]; $D = 0.9$ m from Ref. [49]; and 0.82 m × 0.82 m orifice from Ref. [50].)

sensitive nature of the fuel–air mixtures. These results were obtained with acetylene fuel, but there is no reason to exclude similar phenomena in other fuel–air mixtures provided the scale is sufficiently large. With an initial flame jet velocity of 600 m/s, for example, a critical tube to flame jet diameter $(d_c/D)$
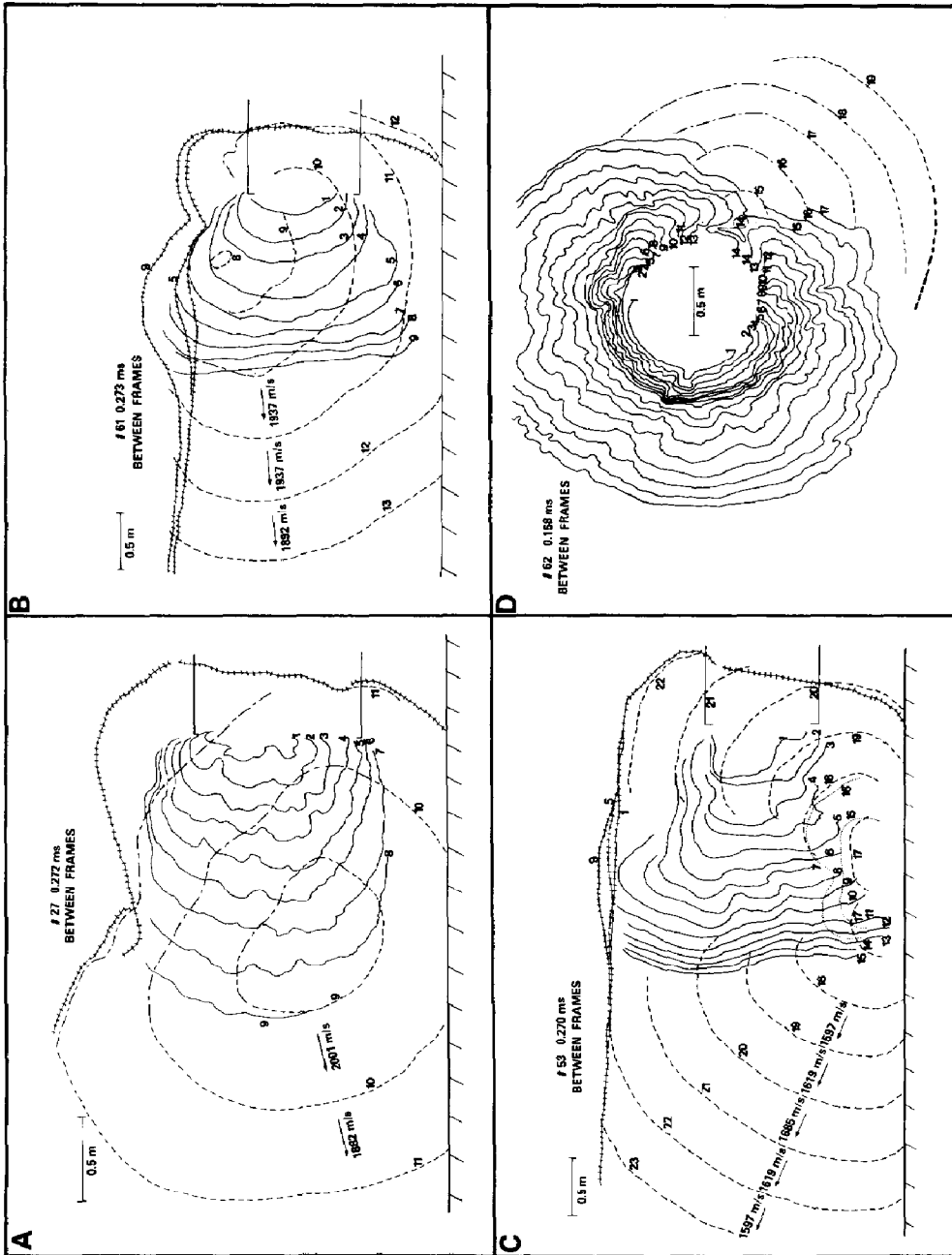
Fig. 19. Flame front and detonation front contour plots taken from the high-speed cinematographic records showing the various modes of transition to detonation: (A) transition in the pre-established flow downstream of a central blockage, (B) transition resulting from a flame/boundary interaction, (C) transition in the wake of the explosion reflecting from the ground, and (D) transition resulting from the collision of flame tongues in an asymmetric flame jet. Solid lines denote flame contours. Dashed lines signify detonation front contours. Cross-hatched lines depict boundaries of the plastic bag [49].

of about 0.1 would be required, as observed in acetylene–air. This corresponds to minimum jet diameters of about 2.0 m, 3.0 m, 9.0 m and 40 m for hydrogen–, ethylene–, propane– and methane–air mixtures, respectively. These scale requirements could be reduced significantly by increasing the flame jet velocity. According to Fig. 18, an increase to 700 m/s, could decrease the minimum flame diameters by a factor of five.

## 6. Conclusions

Several experimental observations of transition to detonation in fuel–air mixtures have clearly demonstrated that transition phenomena, similar to those identified in more sensitive fuel–oxygen mixtures, can also occur in fuel–air mixtures. This means that the worst case detonation scenario cannot be excluded *a priori* in assessing the hazards from vapour cloud explosions.

The obstacle and confinement environment of the vapour cloud must be taken into account in assessing the potential for DDT. Weak ignition of vapour clouds in an unconfined, relatively unobstructed environment is unlikely to result in DDT, even for relatively sensitive fuel–air mixtures. On the other hand, DDT can be considered likely in highly confined clouds, particularly if there are obstacles present to accelerate the flame. Explosions in confined spaces can also serve as strong ignition sources for external clouds, greatly enhancing the potential for DDT. In partially confined regions, more typical of chemical plants, the potential for DDT is less than in the heavily confined regions, and depends critically on the degree of confinement, the obstacle configuration, the ignition source, the initial turbulence and the fuel–air mixture. Any configuration which can produce large turbulent burning pockets or eddies is susceptible to localized explosions which can trigger transition to detonation.

At the present time, it is not possible to predict whether transition can occur in a given spill scenario, but considerable progress has been made towards quantifying both the flame acceleration processes and the relative detonability of fuel–air mixtures. The qualitative 'picture' of the transition phenomena presented by Lee and Moen [11] in 1980 remains essentially unchanged. New data which lend further support to this 'picture' have been described. Of particular relevance are the observations of DDT in large scale experiments. These observations confirm that the essential requirement for transition is a high rate of energy release associated with rapid burning or explosion of a sufficiently large volume. The minimum volume required depends on the sensitivity of the mixture to detonation. This sensitivity can be characterized by the detonation length scales (i.e., the detonation cell size and the critical tube diameter). Typically, the detonation length scales for fuel–air mixtures are at least an order of magnitude larger than those for fuel–oxygen, so that large scale experiments were required to clarify the potential for DDT in fuel–air mixtures.

Quantitative criteria for the critical turbulent mixing and burning rates required for DDT in a given fuel–air mixture are still lacking. However, it has been shown that the critical conditions can be achieved by: (i) flame acceleration; (ii) ignition of a turbulent pocket; and (iii) jet ignition. Better controlled and diagnosed experiments supported by numerical calculations are required to quantify the mechanisms responsible for DDT. Such investigations are particularly important for clarifying the potential for DDT in less sensitive fuel–air mixtures such as methane–air. Since, the scale of the experiments required to confirm this potential becomes prohibitively large (e.g., 10–40 m diameter flame jets for methane–air) it is recommended that extensive fundamental theoretical, numerical and experimental studies of the DDT mechanisms be performed before such experiments are attempted.

# References

1   H. Pförtner and H. Schneider, Explosion von Wasserstoff–Luft Gemischen unter teilverdämmten Bedingungen und unter dem Einfluss einer turbulenten Strömung, FhG-ICI Report, 1984, Pfinztal–Berghausen (FRG).

2   I.O. Moen, D. Bjerketvedt, A. Jenssen and P.A. Thibault, Transition to detonation in a large fuel–air cloud, Combustion and Flame, 61 (1983) 285–291.

3   M.P. Sherman, S.R. Tieszen, W.B. Benedick, J.W. Fisk and M. Carcissi, The effect of transverse venting on flame acceleration and transition to detonation in a large channel, AIAA Prog. Astronaut. Aeronaut. 106 (1986) 66–89.

4   I.O. Moen, A. Sulmistras, B.H. Hjertager and J.R. Bakke, Turbulent Flame Propagation and Transition to Detonation in Large Fuel–Air Clouds, 21st Symp. (Int.) on Combustion, The Combustion Institute, Pittsburgh, PA, 1986, pp. 1617–1627.

5   I.O. Moen, D. Bjerketvedt, T. Engebretsen, A. Jenssen, B.H. Hjertager and J.R. Bakke, Transition to detonation in a flame jet, Combustion and Flame, 75 (1989) 297–308.

6   M. Bjørkhaug and B.H. Hjertager, Influence of obstacle shape, fuel composition and obstacle layout on Flame and Pressure Development in a Radial Vessel of 10 m Radius, Chr. Michelsen Institute Report No. 865403-1, Bergen (Norway), 1986.

7   R.J. Harris and M.J. Wickens, Understanding vapour cloud explosions — An experimental study, Communication 1408, 55th Atumn Meeting of the Institute of Gas Engineers, Kensington Hall Town, 27–28 November, The Institution of Gas Engineers, London, 1989.

8   C.K. Chan, Personal communication, 1991.

9   J.E. Lee, R. Knystautas and N. Yoshikawa, Photochemical initiation of gaseous detonations, Acta Astronautica, 5 (1978) 971–982.

10  R. Knystautas, J.H. Lee, I.O. Moen and H.Gg Wagner, Direct initiation of spherical detonation by a hot turbulent gas jet, 17th Symp. (Int.) on Combustion, The Combustion Institute, Pittsburgh, PA, 1979, pp. 1235–1244.

11  J.H.S. Lee and I.O. Moen, The mechanisms of transition from deflagration to detonation in vapor cloud explosions, Prog. Energy Combust. Sci. 6 (1980) 359–389.

12  J.E. Shepherd and J.H.S. Lee, On the transition from deflagaration to detonation, In: M.Y. Hussaini, A. Kunar and R.G. Voight (Eds.), Major Research Topics in Combustion, Springer-Verlag, Berlin, 1992, pp. 439–487.

13   S. Gordon and B.J. McBride, Computer program for calculation of complex chemical equilibrium compositions, rocket performance, incident and reflected shocks and Chapman Jouget detonations, NASA Report SP-273, Washington, DC, 1976.

14   M. Cowperthwaite and W.H. Zwisler, TIGER Computer program documentation, Stanford Research Institute Publication No. Z106, Stanford, CA, 1973.

15   I.O. Moen, P.A. Thibault and J.W. Funk, Blast waves from non-spherical fuel–air explosions, Proc. of the 8th Int. Symp. on Military Applications of Blast Simulation, Paper No. I.7, Spiez (Switzerland), June 1983.

16   W. Fickett and W.C. Davis, Detonation, University of California Press, Berkeley, CA, 1979.

17   C.K. Westbrook, Chemical kinetics of hydrocarbon oxidation in gaseous detonations, Combustion and Flame, 46 (1982) 191–210.

18   C.K. Westbrook and P.A. Urtiew, Chemical kinetic predictions of critical parameters in gaseous detonations, 19th Symp. (Int.) on Combustion, The Combustion Institute, Pittsburgh, PA, 1982, pp. 615–622.

19   J.E. Shepherd, Chemical kinetics of hydrogen–air–diluent detonations, AIAA Prog. Astronaut. Aeronaut., 106 (1986) 263–293.

20   J.E. Shepherd, I.O. Moen, S.B. Murray and P.A. Thibault, Analyses of the cellular structure of detonations, 21st Symp. (Int.) on Combustion, The Combustion Institute, Pittsburgh, PA, 1987, pp. 1649–1658.

21   I.O. Moen, S.B. Murray, D. Bjerketvedt, A. Rinnan, R. Knystautas and J.E. Lee, Diffraction of detonation from tubes into a large fuel–air explosive cloud, 19th Symp. (Int.) on Combustion, The Combustion Institute, Pittsburgh, PA, 1982, pp. 635–644.

22   I.O. Moen, J.W. Funk, S.A. Ward, M.G. Rude and P.A. Thibault, Detonation length scales for fuel–air explosives, AIAA Prog. Astronaut. Aeronaut., 94 (1983) 55–79.

23   R. Knystautas, C. Guirao, J.H. Lee and A. Sulmistras, Measurement of cell size in hydrocarbon–air mixtures and predictions of critical tube diameter, Critical intiation energy and detonability limits, AIAA Prog. Astronaut. Aeronaut., 94 (1983) 23–37.

24   O. Peraldi, R. Knystautas and J.H. Lee, Criteria for Transition to Detonation in Tube, 21st Symp. (Int.) on Combustion, The Combustion Institute, Pittsburgh, PA, 1988, pp. 1629–1636.

25   R. Knystautas, J.E. Lee, O. Peraldi and C.K. Chan, Transmission of a flame from a rough to a smooth-walled tube, AIAA Prog. Astronaut. Aeronaut., 106 (1986) 37–52.

26   I.O. Moen, A. Sulmistras, G.O. Thomas, D. Bjerketvedt and P.A. Thibault, The influence of cellular regularity on the behaviour of gaseous detonations, AIAA Prog. Astronaut. Aeronaut., 106 (1986) 220–243.

27   T. Engebretsen, Propagation of Gaseous Detonations through Regions of Low Reactivity, Doctoral Thesis, Thermal Energy Division, The Norwegian Institute of Technology, Trondheim (Norway), 1991.

28   G. Dupré, O. Peraldi, J.H.S. Lee and R. Knystautas, Propagation of detonation waves in an acoustic absorbing walled tube, Prog. Astronaut. Aeronaut., 114 (1988) 248–263.

29   Ya.B. Zeldovich, S.M. Kogarko and N.N. Simonov, An experimental investigation of spherical detonation of gases, Sov. Phys.-Tech. Phys., 1 (1956) 1689–1713.

30   D.C. Bull, Concentration limits to the initiation of unconfined detonation in fuel/air mixtures, Trans. Inst. Chem. Eng., 57 (1979) 219–227.

31   W.B. Benedick, C.M. Guirao, R. Knystautas and J.H. Lee, Critical charge for the direct initiation of detonation in gaseous fuel–air mixtures, AIAA Prog. Astronaut. Aeronaut., 106 (1986) 181–202.

32   I.O. Moen and A.J. Saber, Explosion Hazards of Hydrogen Sulphide, Phase II: Flame Acceleration and Transition to Detonation Review, Atomic Energy Control Board Report, Ottawa, Ont., Canada, September 1985.

33   P.A. Urtiew and A.K. Oppenheim, Experimental observations of transition to detonation in an explosive gas, Proc. R. Soc., A295 (1966) 13–28.

34  J.H. Lee, R. Knystautas and C.K. Chan, Turbulent flame propagation in obstacle-filled tubes, 20th Symp. (Int.) on Combustion, The Combustion Institute, Pittsburgh, PA, 1985, pp. 1663–1672.
35  W. Bartknecht, Explosions, Springer-Verlag, Berlin, 1981.
36  H. Steen and K. Schampel, Experimental investigation of the run-up distance of gaseous detonations in large pipes, 4th Int. Symp. on Loss Prevention and Safety Promotion in the Process Industries, Pergamon Press, London, 1983, pp. E23–33.
37  I.O. Moen, J.H.S. Lee, B.H. Hjertager, K. Fuhre and R.K. Eckhoff, Pressure development due to turbulent flame propagation in large-scale methane–air explosions, Combustion and Flame, 47 (1982) 31–52.
38  C. Chan, J.H.S. Lee, I.O. Moen and P.A. Thibault, Turbulent flame acceleration and pressure development in tubes, Proc. 1st Specialist Meeting (Int.) of the Combustion Institute, Bordeaux (France), 20–24 July, 1981, p. 479.
39  B.H. Hjertager, K. Fuhre, S.J. Parker and J.R. Bakke, Flame acceleration of pro-pane–air in a large obstructed tube, AIAA Prog. Astronaut. Aeronaut., 94 (1984) 504–522.
40  B.H. Hjertager, Simulation of transient compressible turbulent reactive flows, Combust. Sci. Technol., 27 (1982) 159–170.
41  B.H. Hjertager, Influence of turbulence on gas explosions, J. Hazardous Mater., 9 (1984) 315–346.
42  B.H. Hjertager, Simulation of gas explosions, Model. Ident. Control, 10(4) (1989) 227–247.
43  M. Berman, A critical review of recent large-scale experiments on hydrogen–air detonations, Nucl. Sci. Eng., 93 (1986) 321–347.
44  C.K. Chan, I.O. Moen and J.H.S. Lee, Influence of confinement on flame acceleration due to repeated obstacles, Combustion and Flame, 49 (1983) 27–39.
45  C.J.M. van Wingerden and J.P. Zeeuwen, Investigation of explosion-enhancing properties of a pipe-rack-like obstacle array, AIAA Prog. Astronaut. Aeronaut., 106 (1984) 53–65.
46  K.H. Orth (Responsible Director), Transition from slow deflagration to detonation, CEC-Research Programme Final Report, Control No. SR-019-80D(B), Technisches Berichtwesen R914/83/045, Kraftwerk Union, Reaktorentwicklung, Erlangen (West Germany), 1983.
47  I.O. Moen and A. Sulmistras, Flame Acceleration and Transition to Detonation in Large Fuel–Air Clouds with Obstacles (U), Suffield Memorandum No. 1159, Defence Research Establishment Suffield, Ralston, Alberta, Canada, April 1986. UNCLASSIFIED.
48  P.A. Urtiew, J. Brandeis and W.J. Hogan, Experimental Study of Flame Propagation in Semiconfined Geometries with Obstacles, Combustion Sci. Technol., 30 (1983) 105–119.
49  D.J. Mackay, S.B. Murray, I.O. Moen and P.A. Thibault, Flame-Jet Ignition of Large Fuel–Air Clouds, 22nd Symposium (International) on Combustion, The Combustion Institute, Pittsburgh, PA., 1988, pp. 1339–1353.
50  H. Pförtner and H. Schneider, Versuche zur Freistrahlzündung Partiell Verdämmter Wasserstoff–Luft im Hinblick auf die Skalierbarkeit des Übergangs Deflagration–Detonation, FhG.ICT Report, 1984, Pfinztal-Berghausen, Germany.